High Time Resolution Astrophysics and ELTs

Andy Shearer
Centre for Astronomy
NUI, Galway
on behalf of the Opticon HTRA network

Chandra/HST - Hester et al, 2002

or we want to observe turbulence

Andy Shearer
Centre for Astronomy
NUI, Galway
on behalf of the Opticon HTRA network

Chandra/HST - Hester et al, 2002

Time sensitivity

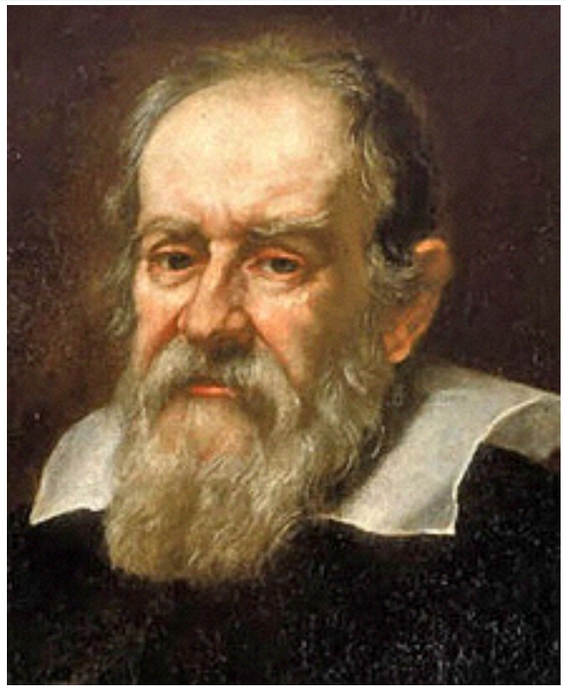

+

τ : ~30 ms
φ : m_V ~ 8.5

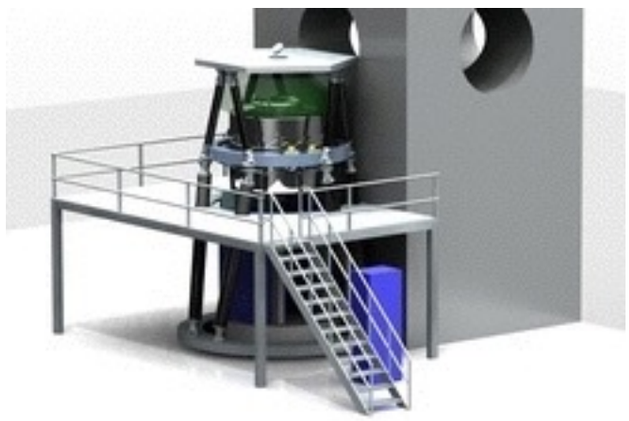

+

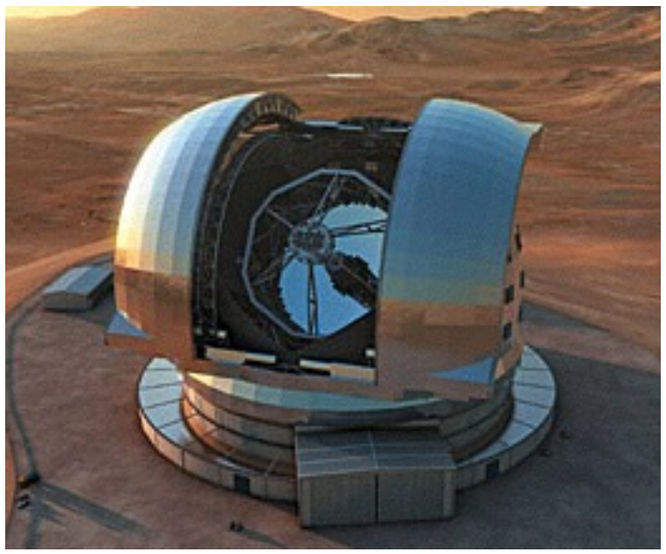

τ ~ 1 hour
φ ~ m_K ~ 30

NUI Galway
OÉ Gaillimh

ETTORE MAJORANA FOUNDATION AND CENTRE FOR SCIENTIFIC CULTURE

OPTICON

CENTRE FOR ASTRONOMY NUI GALWAY

Time sensitivity

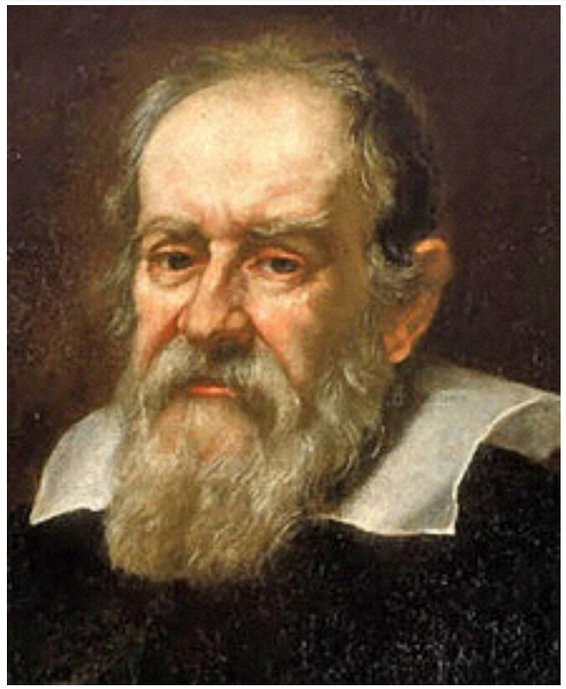

+

τ : ~30 ms

φ : m_V ~ 8.5

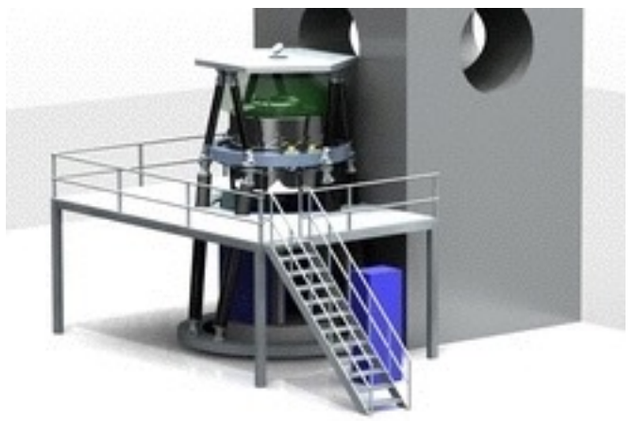

+

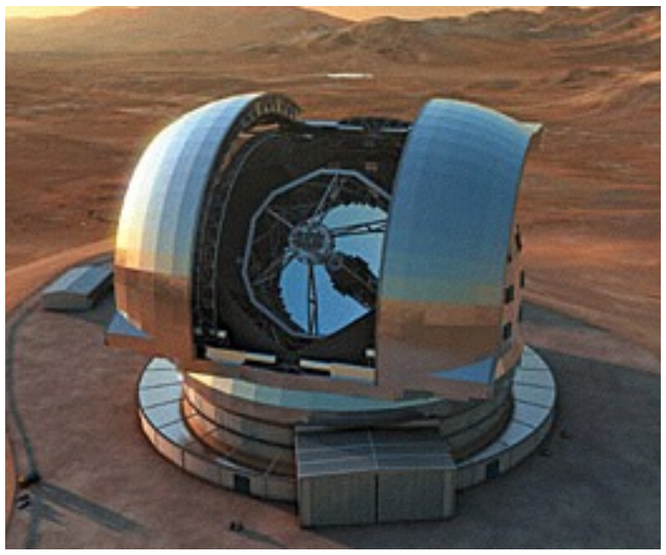

τ ~ 4 ms

φ ~ m_K ~ 18.3

NUI Galway
OÉ Gaillimh

ETTORE MAJORANA FOUNDATION AND CENTRE FOR SCIENTIFIC CULTURE

OPTICON

CENTRE FOR ASTRONOMY NUI GALWAY

Six fundamental questions relating to *extreme physics*

- How did the universe begin?
- What is dark energy and dark matter?
- **Can we observe strong gravity in action?**
- **How do supernovae and γ-ray bursts work?**
- **How do black hole accretion, jets and outflows operate?**
- **What do we learn from energetic radiation and particles?**

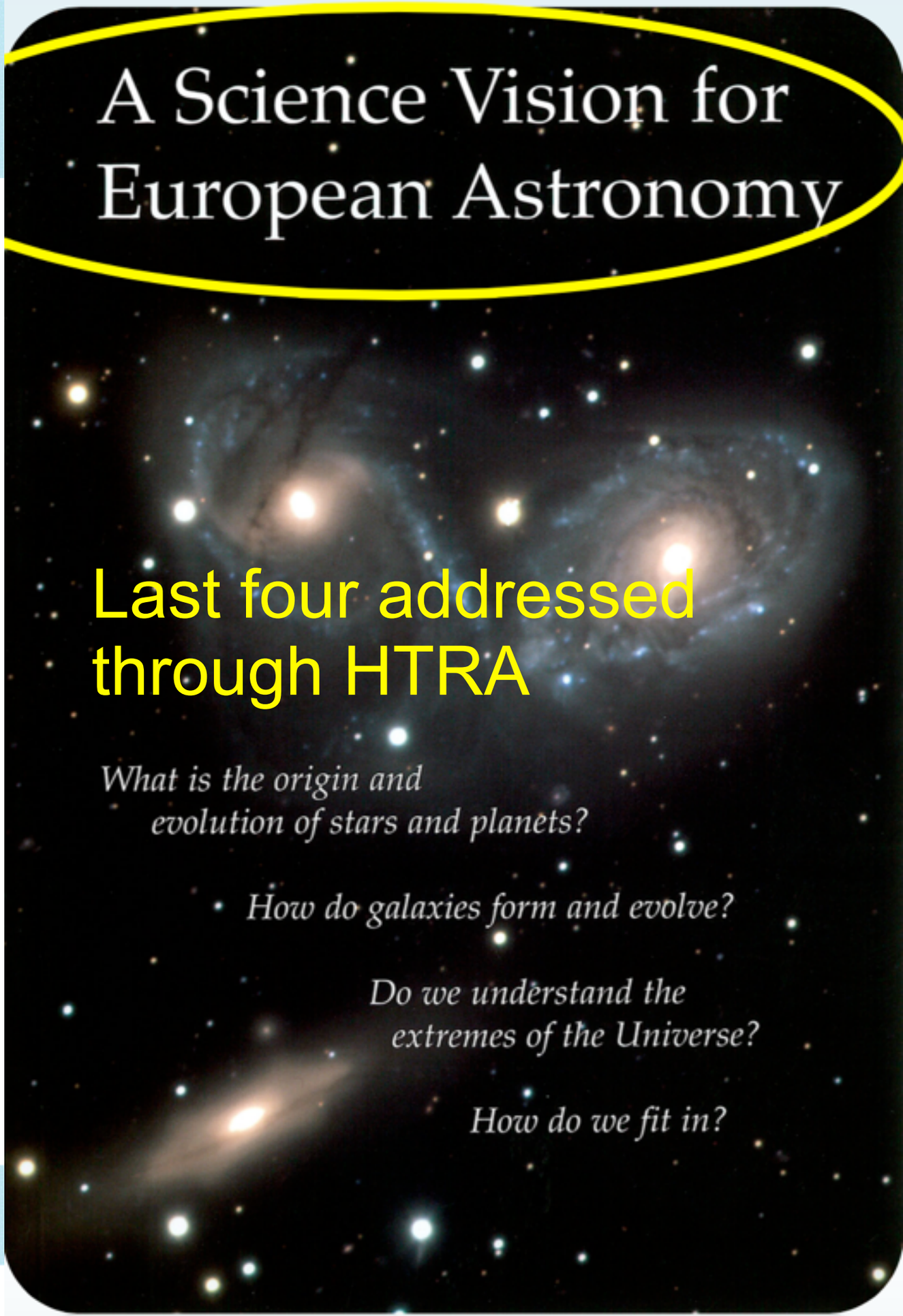

Goes beyond *extreme physics*

- Topics addressed in recent HTRA workshops - see htra.ie for details

  - Binary Systems
  - CVs
  - LMXBs
  - HMXBs
  - Neutron Stars
  - Pulsars, Magnetars, Isolated NS
  - Normal Stars
  - Asteroseismology
  - Stellar Pulsations
  - Brown Dwarfs
  - Transients and Occulations
  - AGN
  - ……..

PROCEEDINGS OF SCIENCE

Shearer et al. 2010, arXiv:1008.0605

High Time Resolution Astrophysics in the Extremely Large Telescope Era : White Paper*

How does SKA1 compare with the world's biggest radio telescopes?

SKA
SQUARE KILOMETRE ARRAY

SKA1 LOW

Australia

419,000m²

~130,000 antennas

MWA

Murchison Widefield Array, Australia

2,500m²

2048 antennas

LOFAR

Low Frequency Array for Radio astronomy, Netherlands

52,000m²

34,000 antennas

GMRT

Giant Metrewave Radio Telescope, India

48,000m²

30 dishes

110 MHz

QUENCIES

SKA1 MID

South Africa

33,

~200

AS

4,

36

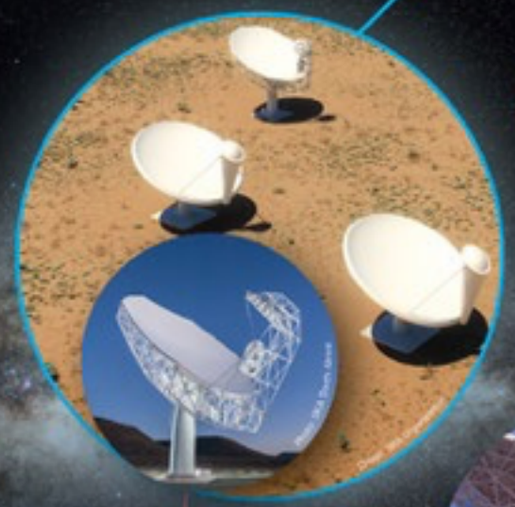

MeerKAT

South Africa

9,000m²

64 dishes

JVLA

Karl G. Jansky Very Large Array, USA

13,200m²

27 dishes

NF

7,

30

ARRAYS

MID FREQUENCIES

FREQUENCIE

quare Kilometre Array (SKA) will be the world's largest radio ope, revolutionising our understanding of the Universe. The SKA will be two phases - SKA1 and SKA2 - starting in 2018, with SKA1 enting a fraction of the full SKA. SKA1 will include two instruments - MID and SKA1 LOW - observing the Universe at different frequencies.

A telescope's capacity to receive faint signals - called sensitivity - depends on its collecting area, the bigger the better. But just like you can't compare radio telescopes and optical telescopes, comparison only works between telescopes working in similar frequencies, hence the different categories above.

The collecting area is just one aspect of a telescope's capability though. Arrays like the SKA have an advantage over single dish telescopes: by being spread over long distances, they simulate a virtual dish the size of that distance and s can see smaller details in the sky, this is called resolution.

XIPE

The X-ray Imaging Polarimetry Explorer

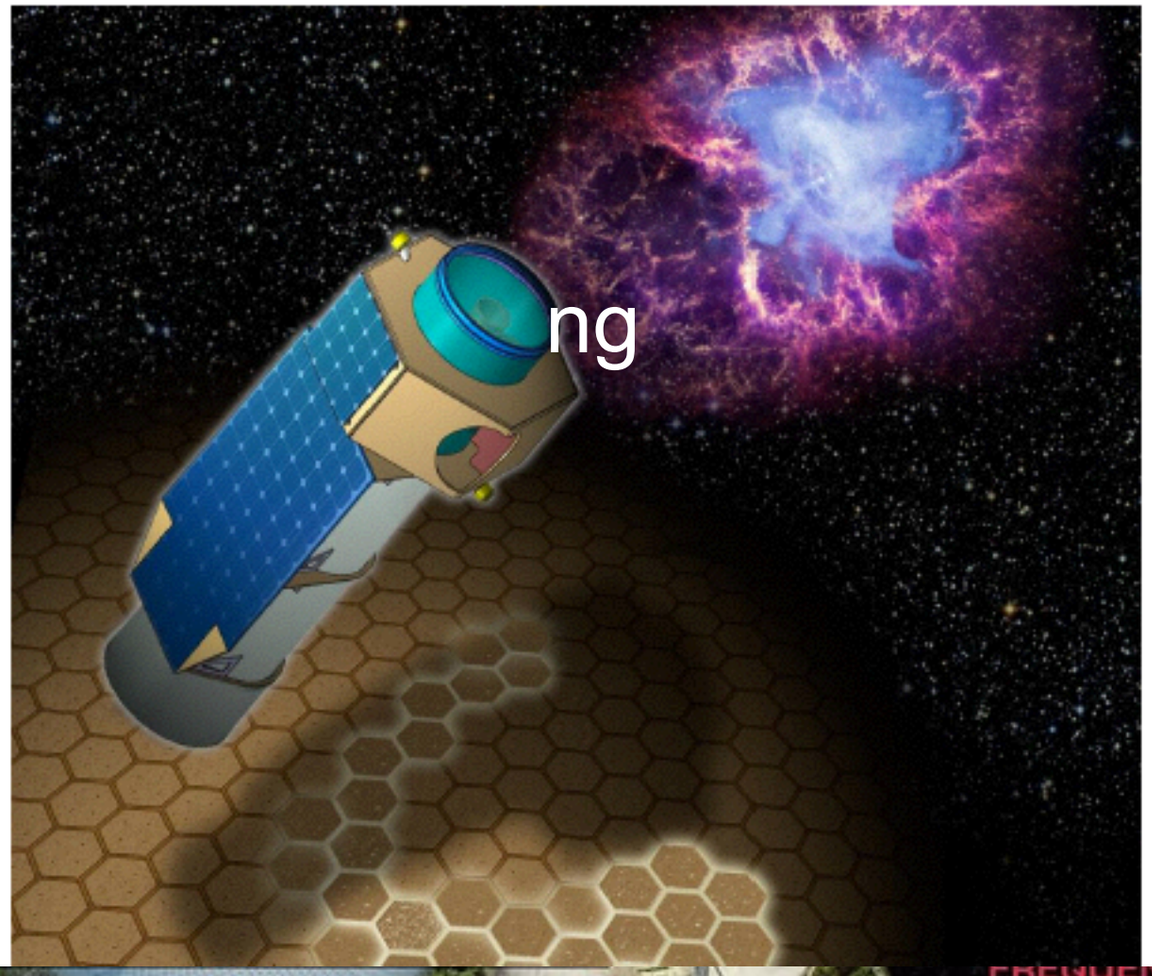

Fermi

Science Support Center

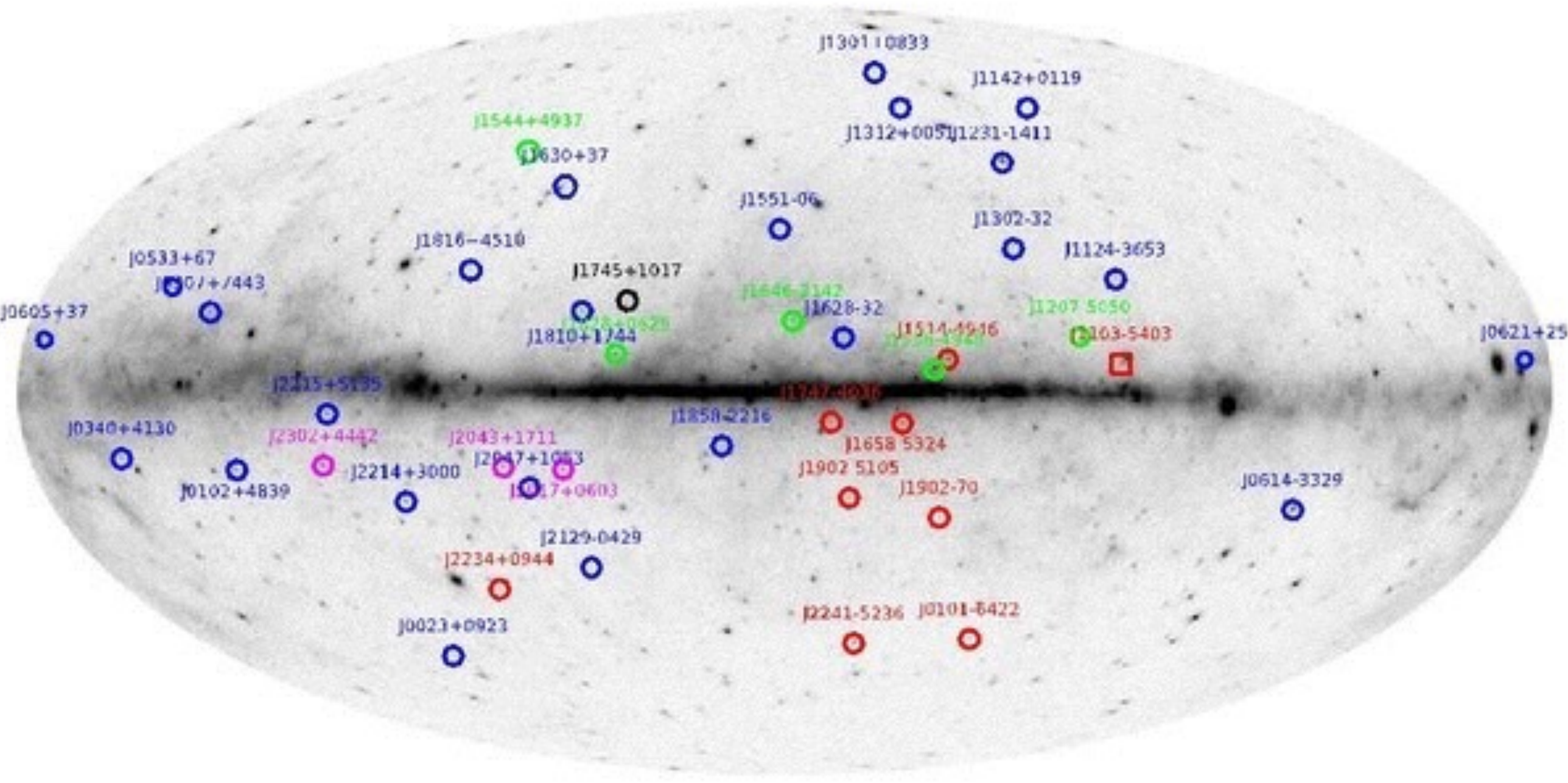

NUI Galway
OÉ Gaillimh

ETTORE MAJORANA FOUNDATION AND CENTRE FOR SCIENTIFIC CULTURE

INAF

OPTICON

ESO

thanks to
G Kanbach

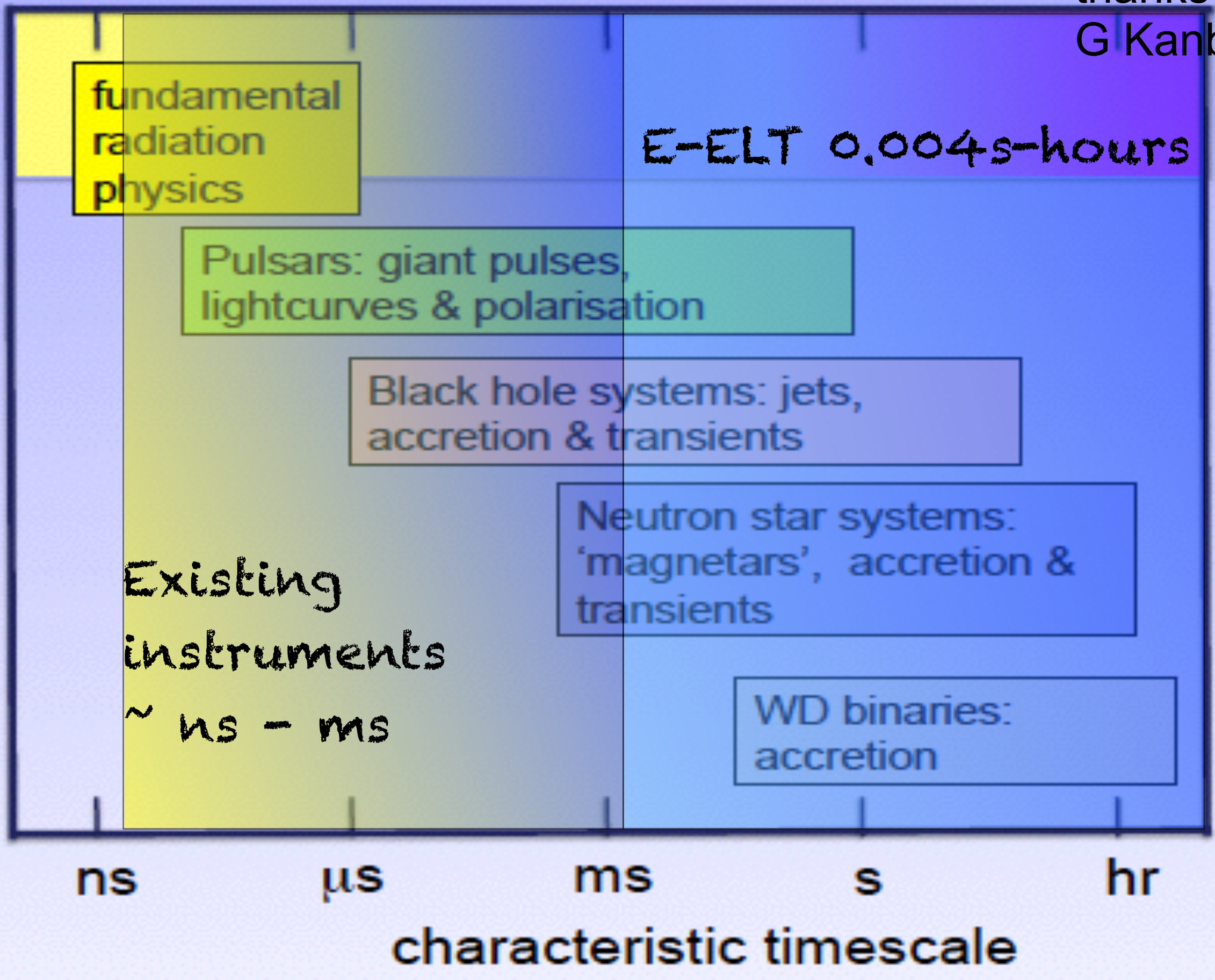

fundamental radiation physics

Pulsars: gia
lightcurves &

Bla
accretion & transients

Neutron star systems: 'magnetars', accretion & transients

WD binaries: accretion

	Radius (km)	Dynamic (s)	Crossing Time (ms)
Sun	700,000	2000	~2,000
White Dwarf	6,000	2	20
Neutron Star	10	0.001	0.03
Pulsar (minimum observed time)	~1m		<2 ns

$$\tau_{dynamic} \sim \sqrt{\frac{R^3}{GM}}$$

$$\tau_{light\ crossing} \sim \frac{R}{c}$$

ns μs ms s hr

characteristic timescale

Is there such a thing as HTRA Science?

- High Time Observations need
  - –fast detectors - **τ ~ μsec, maybe < 1 ns**
  - –low read noise detectors : **n_e = 0**
  - –high quantum efficiency detectors : **DQE ~ 100%**
  - –high photon fluxes :
    - large collecting areas : **ELTs**
    - good throughput : ?

SCIENCE WITH ULTRACAM

see Dhillon, V. S.,et al, 2014, MNRAS, 444, 4021 and Dhillon, V. S.,et al, 2007, MNRAS, 378, 840

~400 nights of time
WHT: 237
NTT: 120
VLT: 40

>80 refereed papers
2 Nature papers
2 Science papers
(3 in the past year)

accreting white dwarfs/cataclysmic variables	19%
black-hole/neutron star X-ray binaries	13%
extrasolar planet transits and eclipses	11%
sdB stars/asteroseismology	11%
eclipsing, detached white-dwarf/red-dwarf binaries	10%
Isolated/non-acccreting white dwarfs	10%
pulsars	6%
flare stars	5%
ultra-compact binaries/double degenerates	5%
occultations by Titan, Pluto, Uranus, Kuiper Belt Objects	4%
isolated brown dwarfs	2%
GRBs	2%
Miscellaneous objects (AGN, contact binaries, etc)	2%

		Time-scale (now)	Time-scale (ELT era)
Stellar flares and pulsations		Seconds/ Minutes	10-100ms
Stellar surface oscillations	White Dwarfs Neutron Stars	1-1000 μsec	1-1000 μsec 0.1 μsec
Close Binary Systems (accretion and turbulence)	Tomography Eclipse in/egress Disk flickering Correlations (e.g. X-ray & optical)	100ms++ 10ms+ 10ms 50ms	10 ms+ < 1ms < 1ms <1ms
Pulsars	Magnetospheric Thermal	1μsec-100ms 10 ms	nsec(?) <ms
AGN		Minutes	Seconds(?)

Instrument	Detector	Group	τ (ms)	Type
UltraCam	Frame Transfer	Sheffield/ Warwick	5ms	Imager (3-Band)
UltraSpec	EMCCD	Sheffield/ Warwick	1ms	Spectrograph
GASP	EMCCD	Galway	600μs	Polarimeter
Optima	APD	MPE	1 ns	Photoncounter / polarimeter
Iqueye	APD	Padua	0.1 ns	Photon counter
Arcons	MKID	UCSB	20 ns	Imager

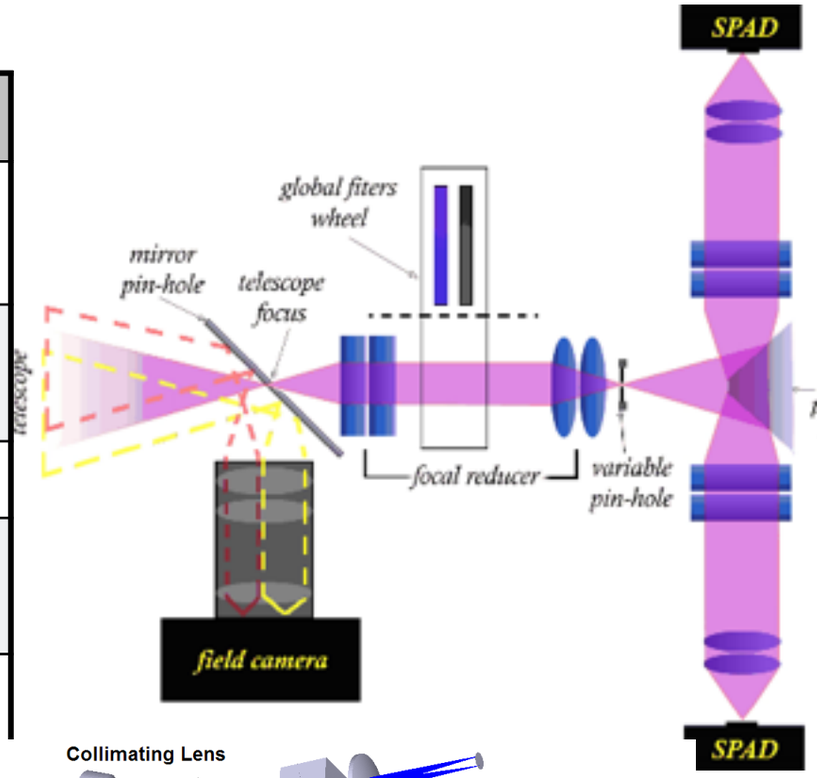

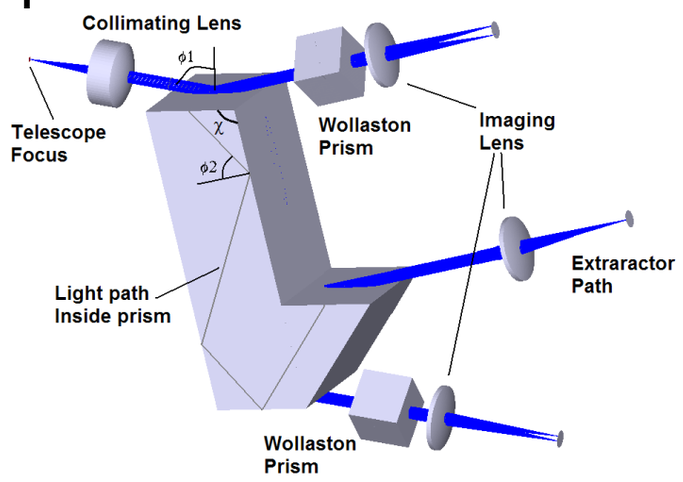

ESO - HTRA : Richichi et al 2009

Instrument	Modes	Detector	Time Rate (Window)
VISIR	Burst	DRS	12.5 ms SF
SOFI	Burst, FastPhot	Hawaii	4 ms (8 x 8), 15 ms (32 x 32)
ISAAC	Burst, FastPhot	Hawaii-1, Aladdin	3 ms (32 x 32), 6 ms (64 x 64)
ISAAC	Burst	Hawaii-1, Aladdin	9 ms (1024 x16)
NACO	Cube	Aladdin	7.2 ms (64 x 64), 350 ms (1024 x 1024)
HAWK-I	Fast	Hawaii-2RG	6.3 ms (16 x 16)
FORS2	HIT	CCD (charge shift)	up to 2.3 ms
VLTI	Fast	Various	up to 1 ms

HTRA Example - pulsars

Pulsars - despite nearly fifty years and a promising start.

Observation of a Rapidly Pulsating Radio Source

by

A. HEWISH
S. J. BELL
J. D. H. PILKINGTON
P. F. SCOTT
R. A. COLLINS

Mullard Radio Astronomy Observatory,
Cavendish Laboratory,
University of Cambridge

Unusual si
the Mullar
come from
with oscill

In July
quency
Radio
designed
radio so
the irre

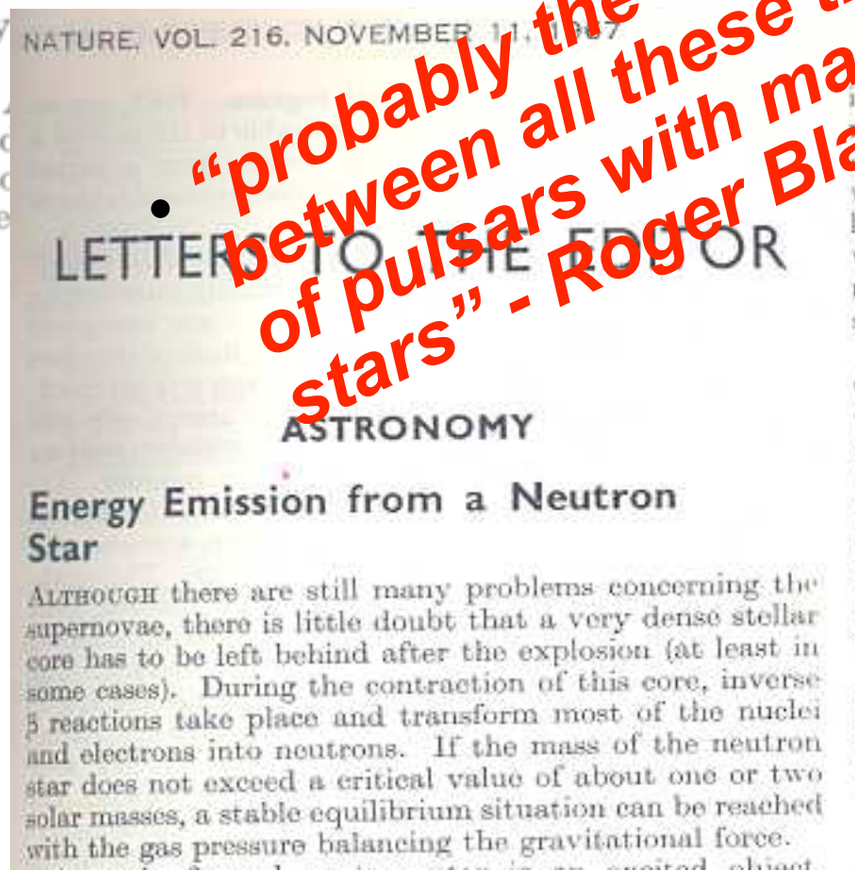
NATURE, VOL. 216, NOVEMBER 11, 1967

LETTERS TO THE EDITOR

ASTRONOMY

Energy Emission from a Neutron Star

ALTHOUGH there are still many problems concerning the supernovae, there is little doubt that a very dense stellar core has to be left behind after the explosion (at least in some cases). During the contraction of this core, inverse β reactions take place and transform most of the nuclei and electrons into neutrons. If the mass of the neutron star does not exceed a critical value of about one or two solar masses, a stable equilibrium situation can be reached with the gas pressure balancing the gravitational force.

- "probably the only point of agreement between all these theories is the association of pulsars with magnetized, rotating neutron stars" - Roger Blandford 1998

NATURE, VOL. 219, JULY 13, 1968

LETTERS TO THE EDITOR

PHYSICAL SCIENCES

Rotating Neutron Stars, Pulsars and Supernova Remnants

I SHALL discuss here some problems connected with theories linking the pulsars to the rotation of neutron stars (ref. 1 and a preprint by L. Woltjer). Because neutron
their r
gaseous
therefo
in the
Gold
detecti
very d
It is al
if the
rotatio
individ
present
for a pulsating radio source in this part of the sky (Drake,

cm². Tl
that is,
neutron
Sun th
uncerta
star ca
emphas
the gas
sibility
star ma
tion of
I sha
a neutr
quasi-v
of the s
in the
limit c

THE ASTROPHYSICAL JOURNAL, 164:529–556, 1971 March 15

A MODEL OF PULSARS

P. A. STURROCK
Applied Physics Department, Institute for Plasma Research,
Stanford University, Stanford, California
Received 1970 June 22

Let

HTRA Example - pulsars

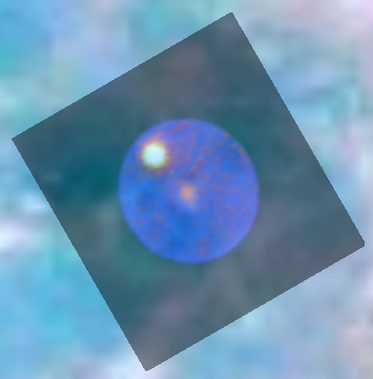

f ~ 30 Hz

Name		Year	Age	mag	D(kpc)	A_V	Phot	Spec	Pol	Tim	Astrom
Crab	F	1969	3.10	16.5	1.73	1.6	UVOIR	Y	Y	P	PM
B1509-58	F	2000	3.19	26	4.2	5.2	OIR		UL*		
B0540-69		1984	3.22	22	49.4	0.6	OIR	Y	Y*	P	PM (UL)
J0205+6449	*F*	*2013*	*3.73*	*27.4*	*2*	*2.5*	*O*				
J1357- 6429	*F*	*2012*	*3.86*	*24.6*	*2.4*	*2.2*	*O*				
Vela	F	1976	4.05	23.6	0.23	0.2	UVOIR	Y	Y*	P	PM,PAR
B0656+14	F	1988	5.05	25	0.29	0.09	UVOIR	Y	Y	P	PM
Geminga	F	1984	5.53	25.5	0.16	0.07	UVOIR	Y		P	PM,PAR
B1055-52	F	1997	5.73	24.9	<0.72	0.22	UVO				PM
B1929+10		1996	6.49	25.6	0.33	0.15	UV				PM
B0950+08		1996	7.24	27.1	0.26	0.03	UVO				
B1133+16		*2008*	*6.69*	*28*	*0.35*	*0.12*	*O*				
J0108-1431		*2008*	*8.3*	*27.*	*0.3*	*0.05*	*O*				
J0437-471	F	2004	9.20	24.8	0.14	0.11	UV	Y			
J1308.6+2127		2002	6.17	28	<1	0.14	O				
J0720-3125		1998	6.27	26.7	0.35	0.10	O				PM,PAR
J1856-3754		1997	6.60	25.7	0.14	0.12	O	Y			PM,PAR
J1605.3+3249		2002	-	27.2	<1	0.06	O				PM
RBS1774		2008	-	27.4	<0.5	0.2	O				
J0806-4123		2011	>6.5	27.9	<0.5	0.1	O				
SGR1806-20		2004	3.14	20.1	15	29	IR				
1E 1547.0-5408		2009	3.14	18.5	9	17	IR		Y*		
1E 1048.1-5937		2004	3.63	21.3	3	6.1	OIR		UL*	P	
XTE J1810-197		2004	3.75	20.8	4	5.1	IR		UL*		
SGR 0501+4516		2009	4.1	19.1	~2	5	IR			P	
4U 0142+61		2002	4.84	20.1	>5	5.1	OIR			P	
1E 2259+586		2002	5.34	21.7	3	5.7	IR				

Thanks to R Mignani

* phase-averaged

	m_B	period (ms)	B photon Fluxes photons/rotation	
			VLT	EELT
Crab	17.2	33	22,801	64,000
Vela	23.6	89	221	475
PSR 0540-69	22.5	50	332	734
PSR 0656+14	25.5	385	11.5	357
Geminga	26.2	237	0.55	1.25
PSR B0950+08	27.1	253	0.22	0.54
PSR B1929+10	25.6	227	0.8	1.92
PSR B1055-52	24.9(U)	197	1.41	3.28
PSR B1509-58	25.7	151	0.55	1.17
PSR B1113+16	28.1	1188	0.44	1.01
Crab at M31	29.7	33	0.00012	0.056

The fastest time-scale - radio observations

Hankins et al Nature, 2003, 422, 141

Structure at 3 nsec level

(resolving 1m at 2 kpc)

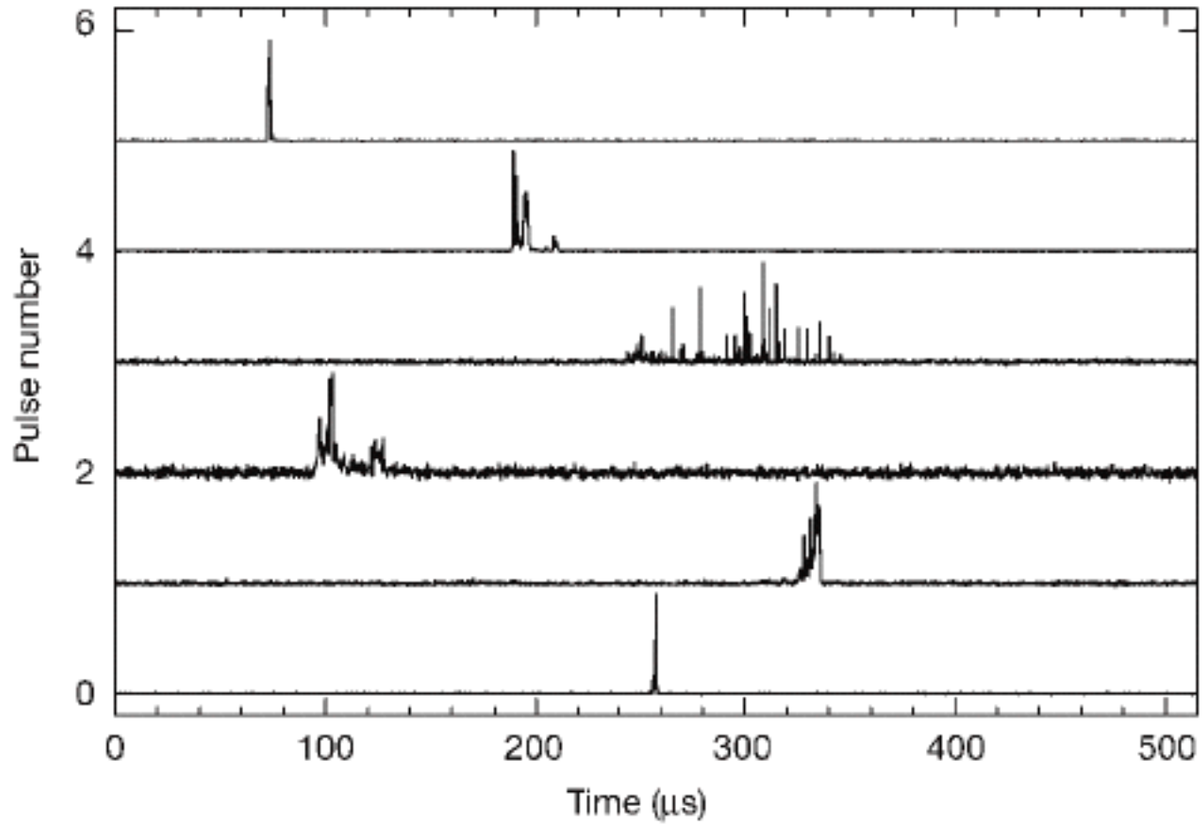

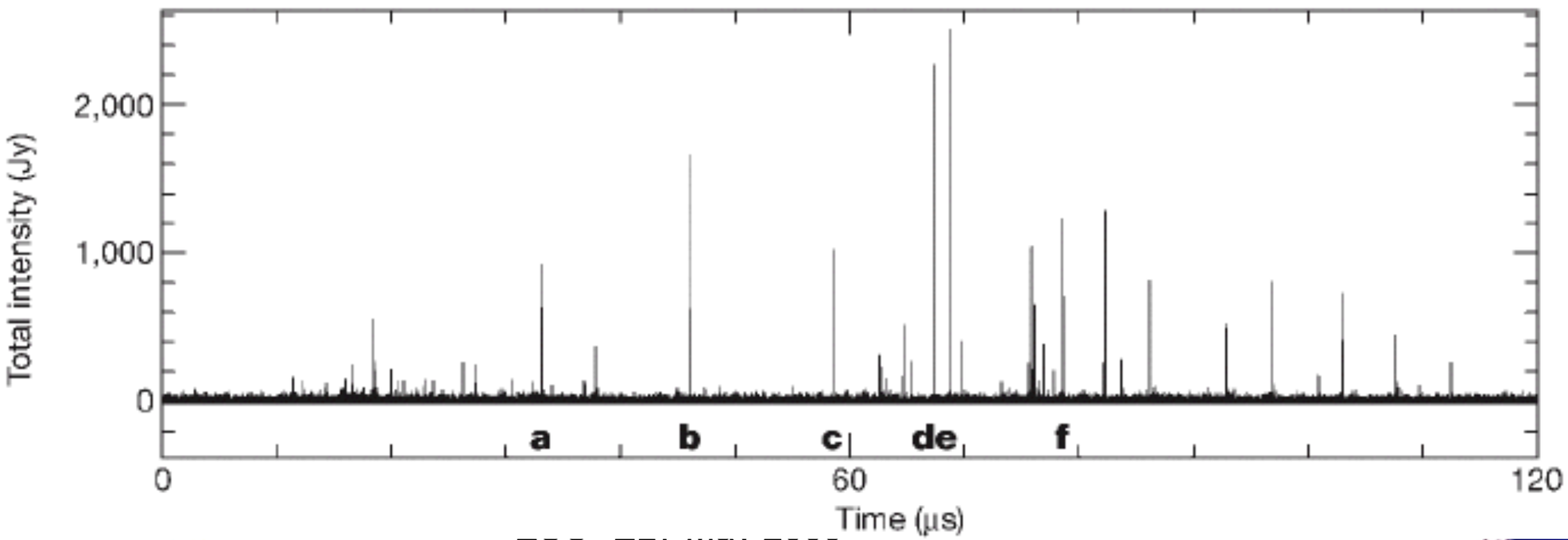

High Energy Emission

Three options

- Synchrotron - optical
- Curvature - γ-ray
- Inverse Compton in polar gap models

The first two apply to the outer and slt gap

Outer gap models describe most high energy emission characteristics but have to explain existence of an outer gap and account for radio emission from the polar gap

But Fermi results rule out Polar Cap

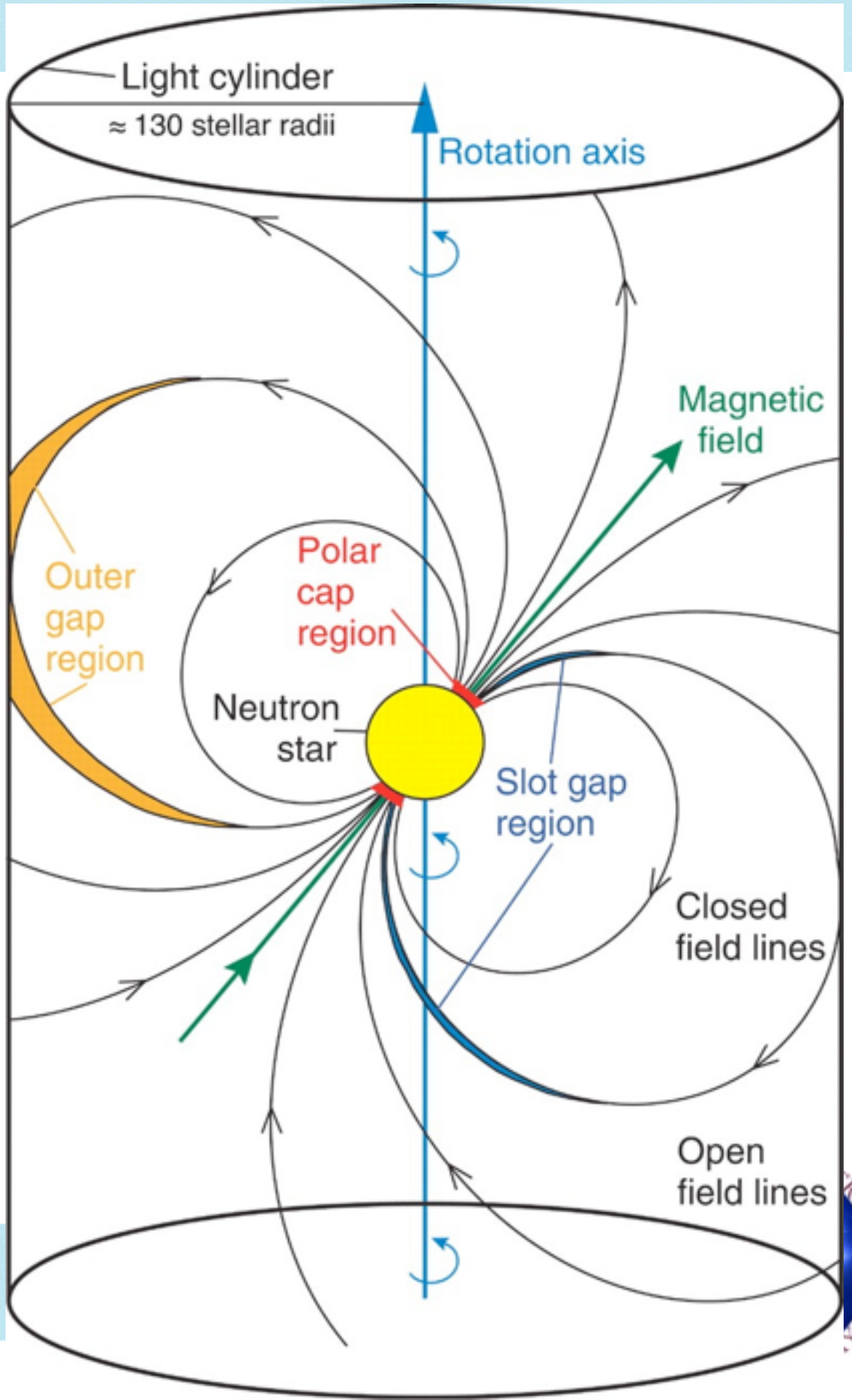

What slows the pulsar down?

Pulsars have a strong surface magnetic field - assumed to be dipolar [it isn't]

A rotating magnetic dipole with moment |**m**| radiates electromagnetic

The electromagnetic power, $\dot{E}_{dipole} = \frac{2}{3c^3}|\mathbf{m}|^2 \Omega^4 \sin^2\alpha$

If $\dot{E}_{dipole} \approx \dot{E}_{spin\ down}$ then

$$\frac{2}{3c^3}|\mathbf{m}|^2 \Omega^4 \sin^2\alpha = -I\Omega\dot{\Omega} \Rightarrow |\mathbf{m}| \propto \sqrt{P\dot{P}}$$

$$\dot{\Omega} = \frac{2|\mathbf{m}|^2 \sin^2\alpha}{3Ic^3}\Omega^3 \text{ or more generally } \propto \Omega^n$$

Or in terms of the frequency ν=1/p

$\dot{\nu}$=-Kν^n, n is the **braking index**

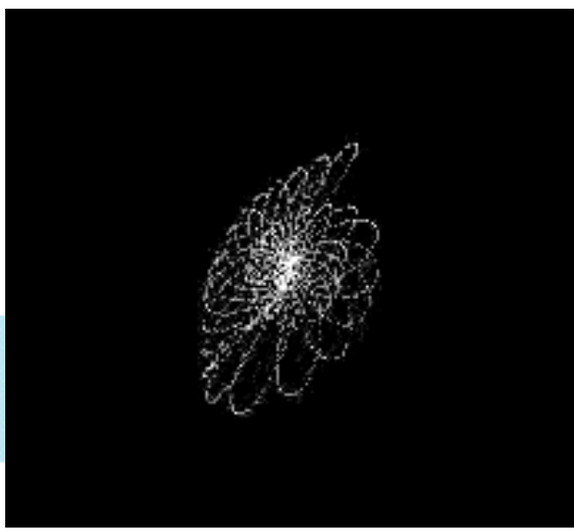

Very basic geometry

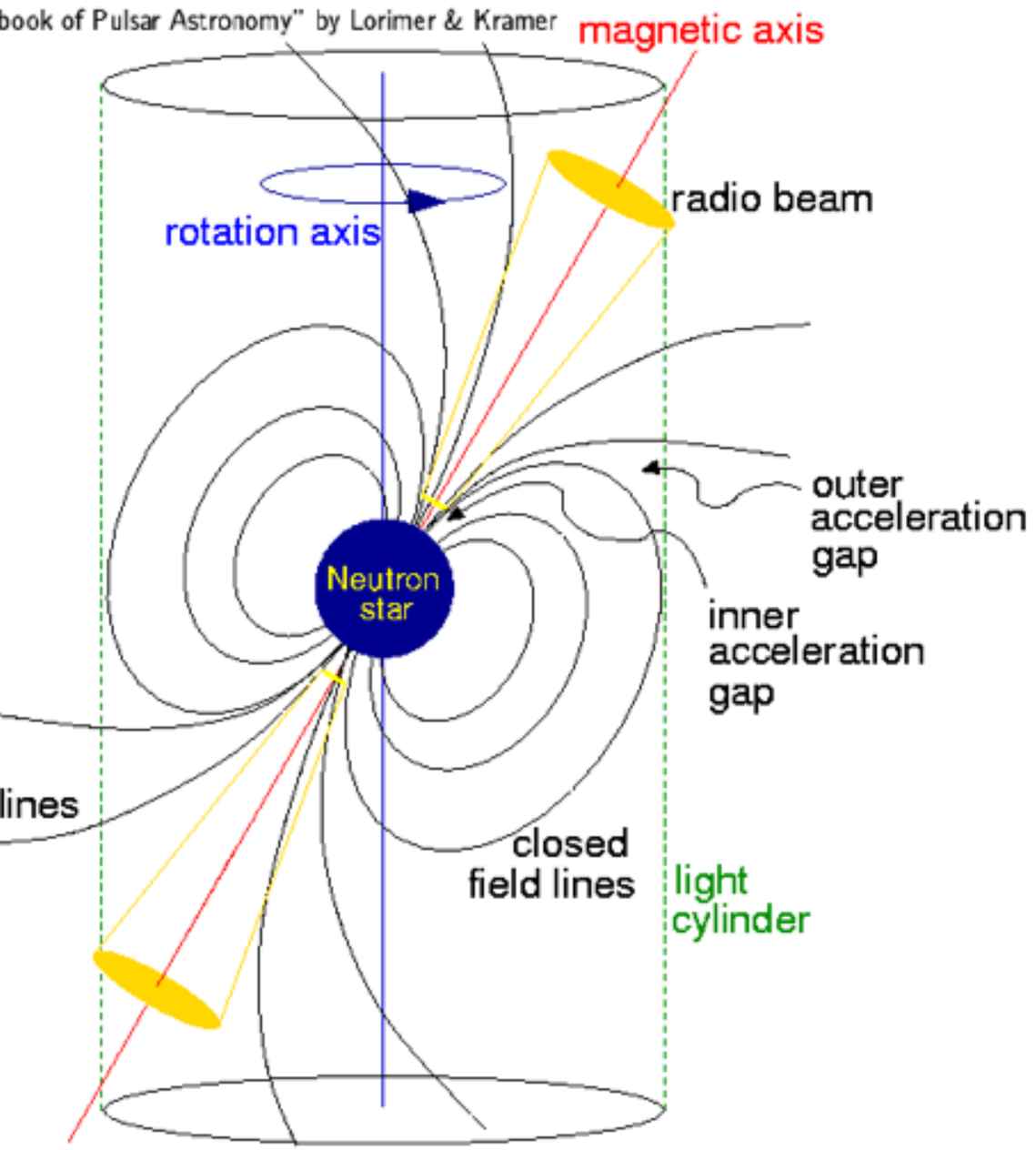

Light Cylinder Radius

$$R_{LC} = \frac{c}{\Omega} = \frac{cP}{2\pi} \simeq 4.8 \times 10^4 \left(\frac{P}{s}\right) km$$

and the magnetic field strength at R_{LC} is

$$B_{LC} = B_S \left(\frac{R}{R_{LC}}\right)^3 \simeq 9.2 \left(\frac{P}{s}\right)^{-5/2} \left(\frac{\dot{P}}{10^{-15}}\right) G$$

Magnetic Field Strength, $B_r \approx |\mathbf{m}| / r^3$

Surface field, $B_s = B_{r=R} = \sqrt{\frac{3c^3 I}{2\pi^2 R^6} P\dot{P}}$

assuming R=10 km and I = 10^{45} g cm^2

$$\mathbf{B_S = 3.2 \times 10^{19} G \sqrt{P\dot{P}} \approx 10^{12} G \left(\frac{\dot{P}}{10^{-15}}\right)^{1/2} \left(\frac{P}{s}\right)^{1/2}}$$

$$\boldsymbol{Characteristic\ Age, \tau = \frac{P}{2\dot{P}}}$$

P-P diagram

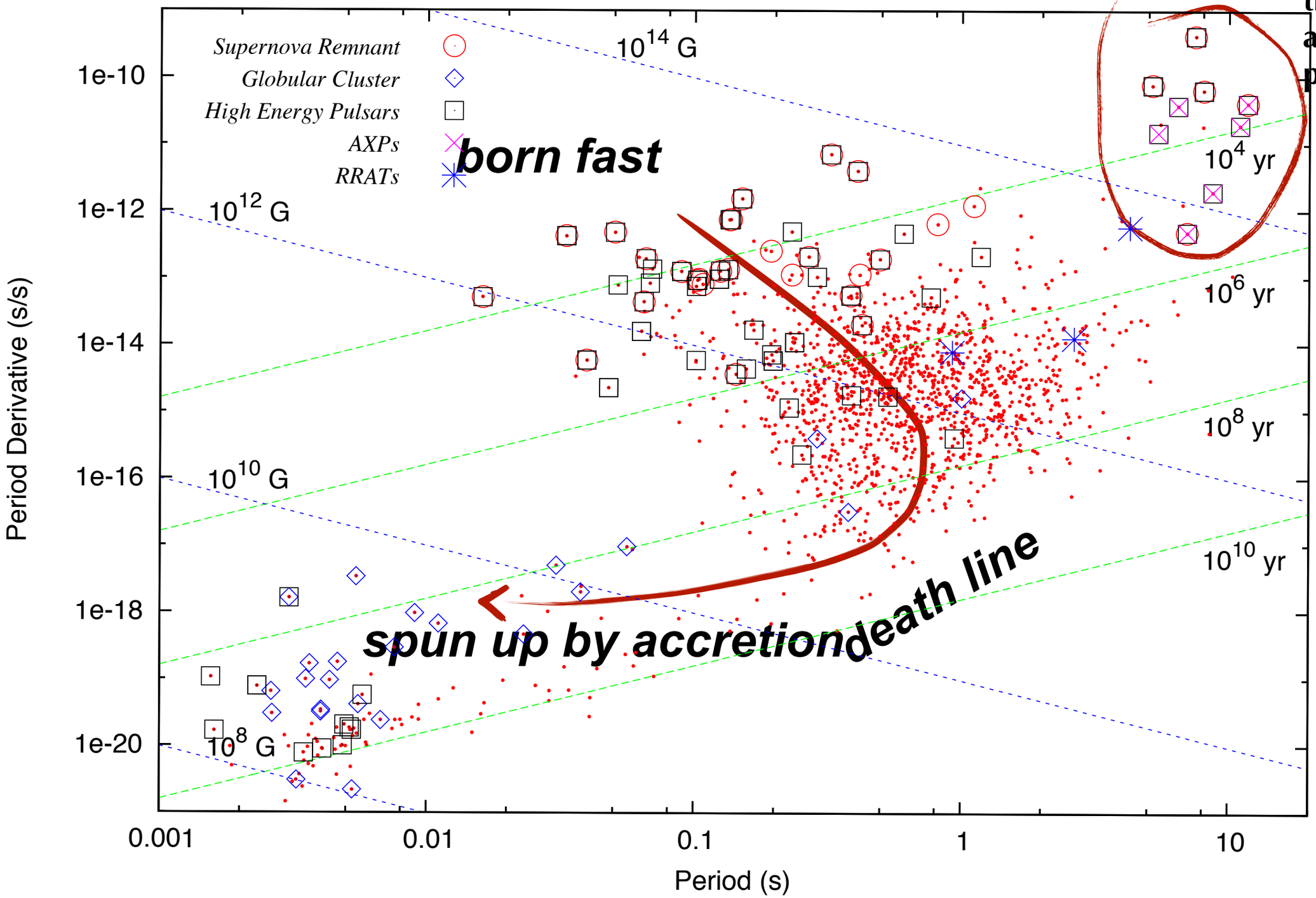

what about these magnetars or anomolous X-ray pulsars - IR objects

see Chen and Ruderman (1993)

taken from Harding - “Neutron Star Zoo” 1302.0869

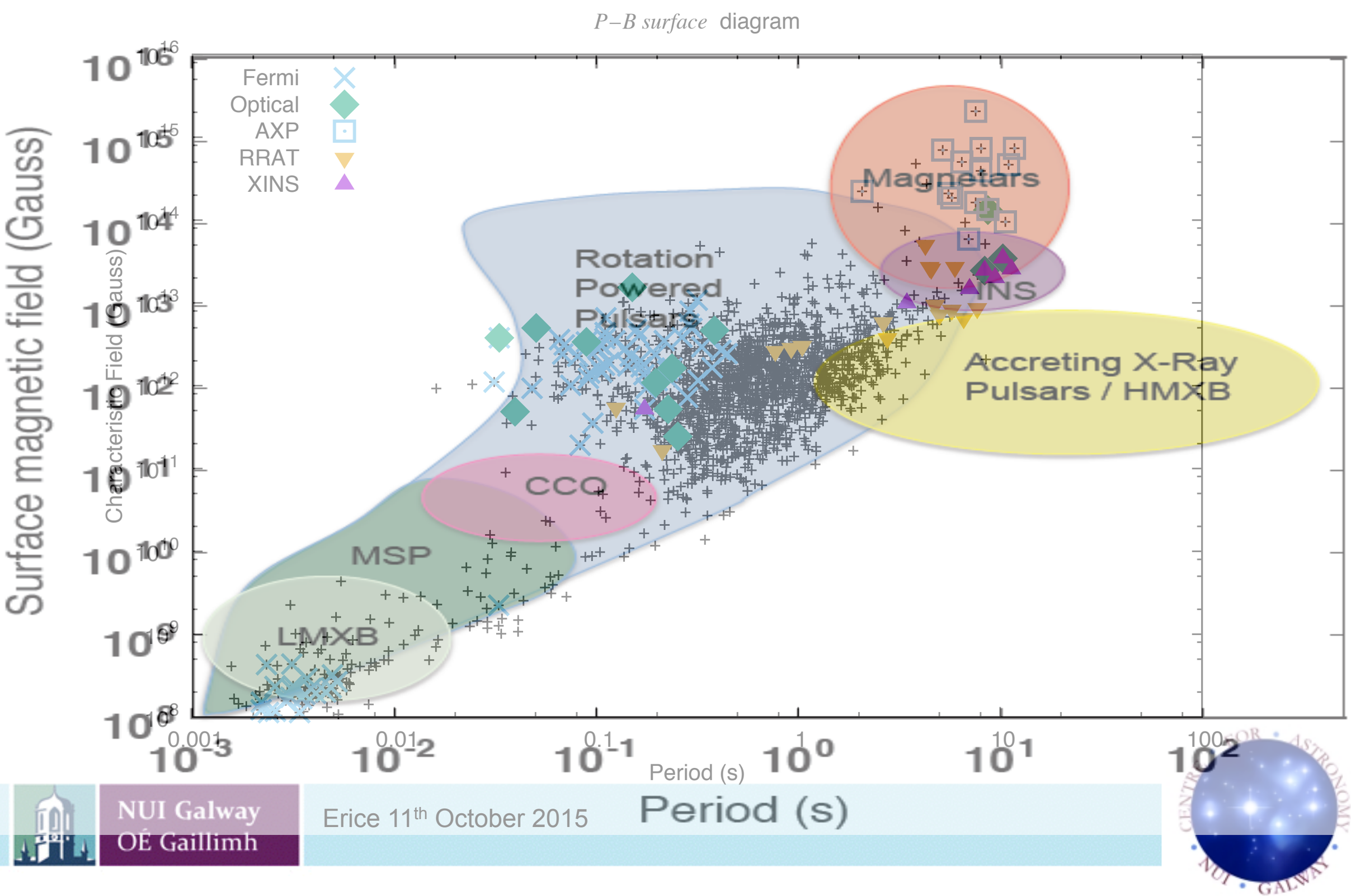

Optical Pulsars - Position on the $P\dot{P}$ diagram

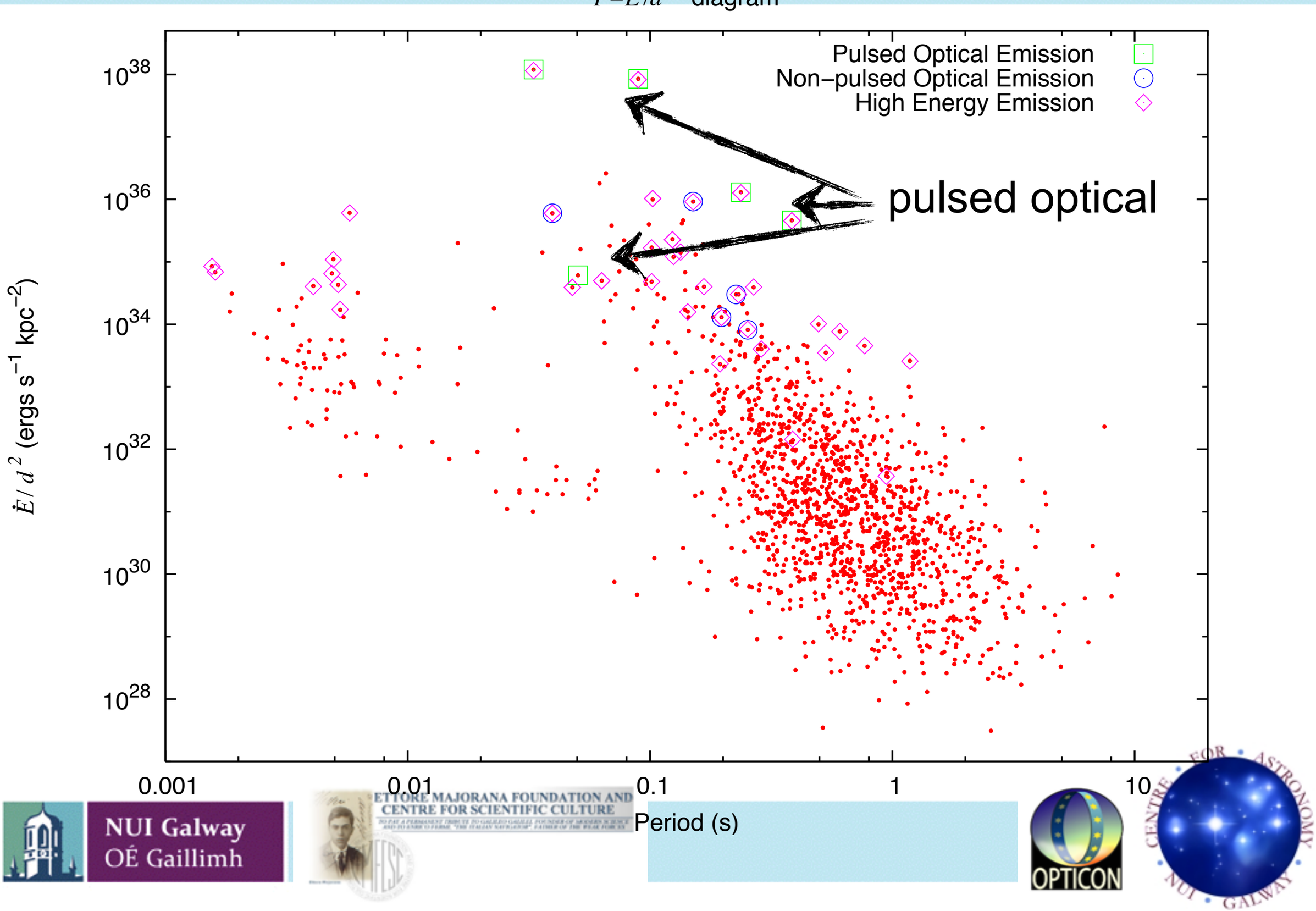

NUI Galway
OÉ Gaillimh

ETTORE MAJORANA FOUNDATION AND CENTRE FOR SCIENTIFIC CULTURE

OPTICON

CENTRE FOR ASTRONOMY NUI GALWAY

Optical Pulsars - the problem

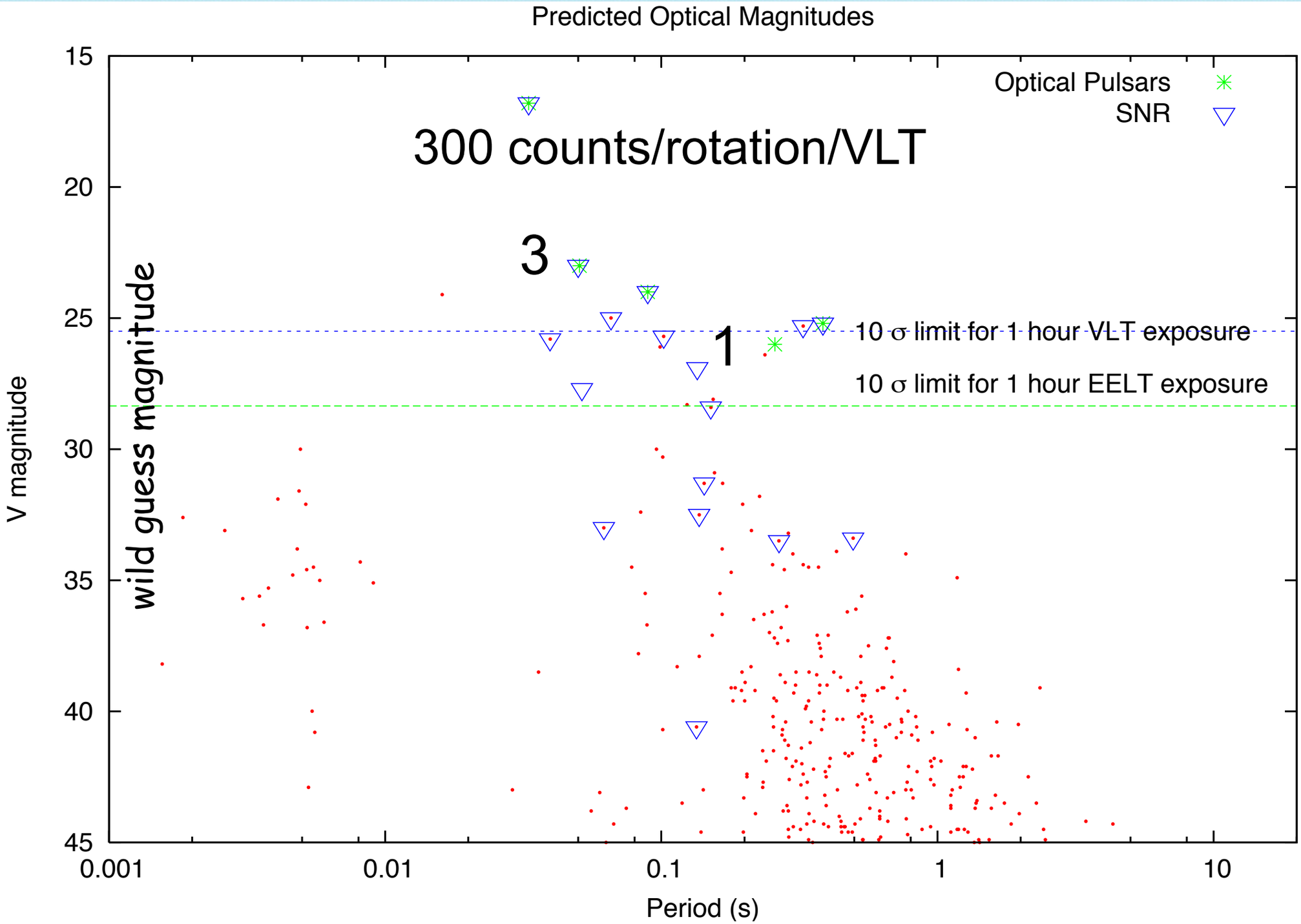

Pulsars - Polarisation

Słowikowska et al., 2009

Table 1. High energy polarisation measurements of pulsars and their nebulae. Polarisation degree is given as a percentage, and position angle in degrees (North, 0° to East, 90°).

Band	Pulsar / Polarisation	Nebula (near PSR)	Ref.
	Crab		
Optical (V$\sim$ 16.6)	phase-resolved (Fig. 4) phase-averaged $9.8\% \pm 0.1\%$ and $109.5° \pm 0.2°$	$9.7\% \pm 0.1\%$; $139.8° \pm 0.2°$ ($< 5''$ from PSR)	[1], [2], [3]
UV	phased-resolved, similar to optical - P.D. and P.A. (MP and IP)		[4]
X-ray	only upper limits	$19.2\% \pm 0.9\%$; $155.8° \pm 1.4°$	[5], [6]
Hard X-ray/ soft γ-ray	off-pulse (phase: 0.52–0.88) $> 72\%$; $120.6° \pm 8.5°$		[7]
	phase-averaged $47\%^{+19\%}_{-13\%}$; $100° \pm 11°$		[7]
γ-ray	off-pulse (phase: 0.5–0.8) $46\% \pm 10\%$; $123° \pm 11°$		[8]
	B0540-69		
Optical (V$\sim$ 22.5)	phase-averaged: $\sim 5\%$, no error quoted; phase-resolved: $< 15\%$	$5.6\% \pm 1.0\%$; $79° \pm 5°$	[9], [10], [11]
	Vela		
Optical (V$\sim$ 23.6)	phase averaged: $9.4\% \pm 4\%$, $146° \pm 11°$		[9], [12]
	B0656+14		
Optical (V$\sim$ 25)	double peak light curve; P.D. bridge $\sim 100\%$, peaks $\sim 0\%$ P.A. sweeps in agreement with RVM		[13]
	B1509-58		
Optical (V$\sim$ 25.7)	phase-averaged: $\sim 10.4\%$ (very uncertain, no error quoted)		[9]

[1] Smith et al. (1988), [2] Słowikowska et al. (2008), [3] this paper, [4] Graham-Smith et al. (1996), [5] Silver et al. (1978), [6] Weisskopf et al. (1978), [7] Forot et al. (2008), [8] Dean et al. (2008), [9] Wagner & Seifert (2000), [10] Middleditch et al. (1987), [11] Chanan & Helfand (1990), [12] Mignani et al. (2007), [13] Kern et al. (2003),

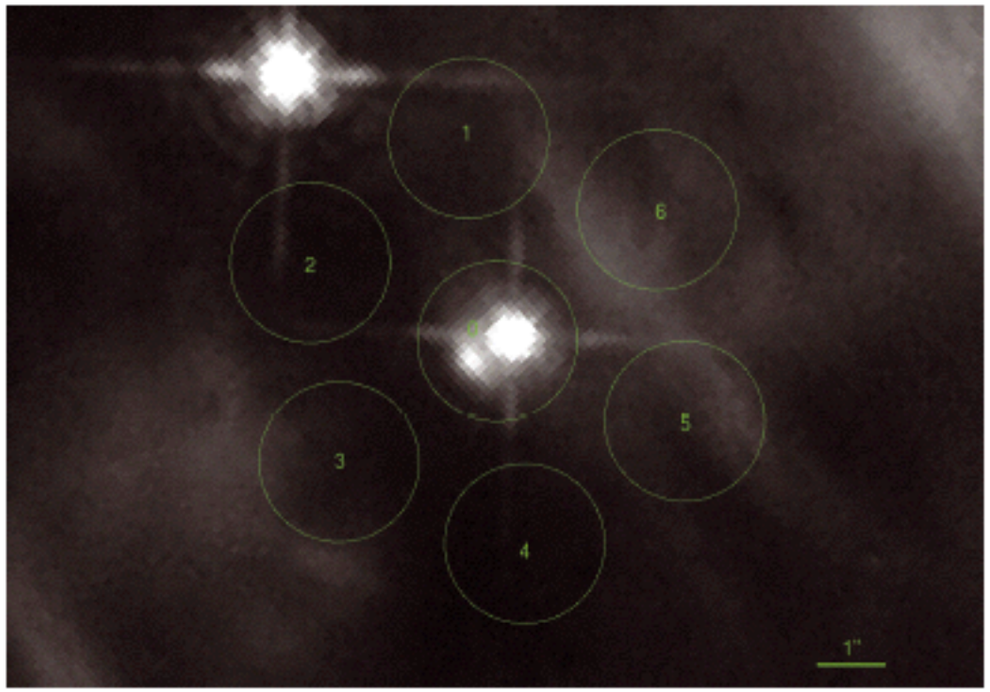

Słowikowska et al 2009

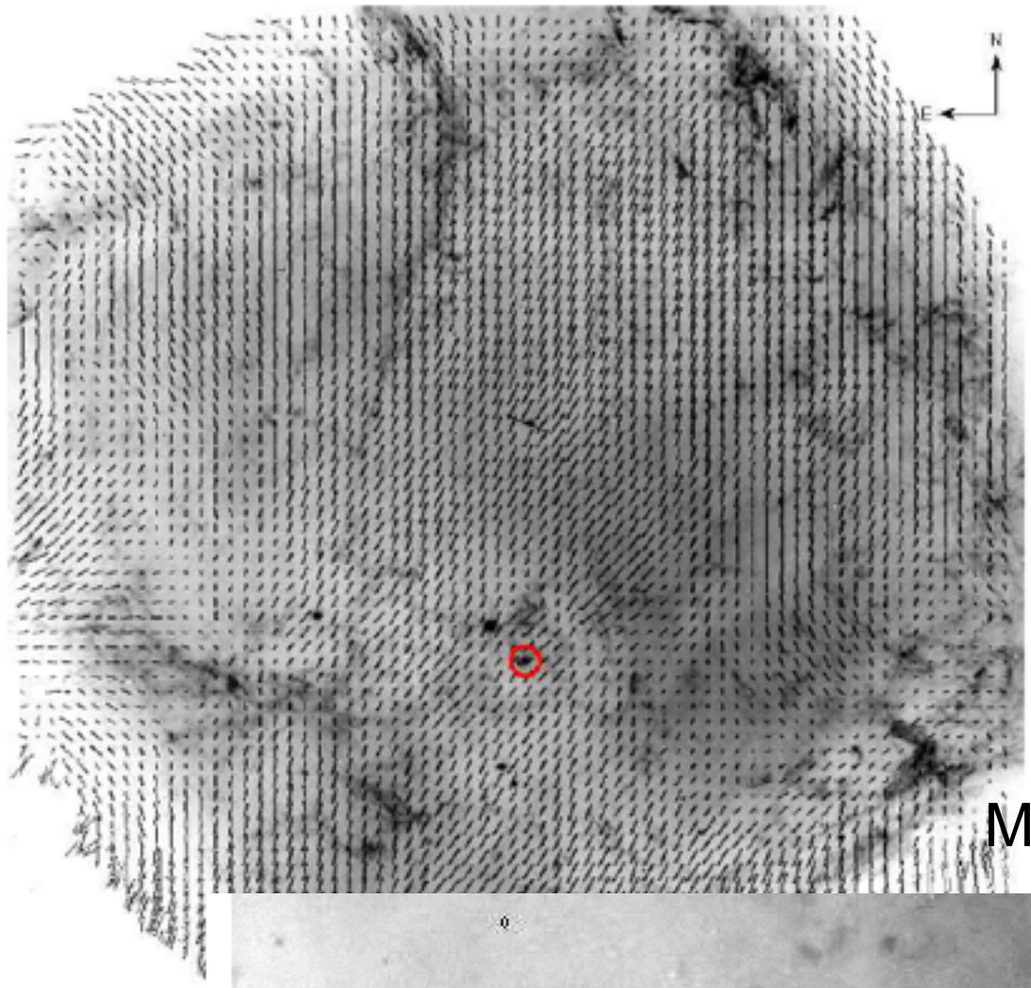

Moran et al, 2013

Moran et al, 2015, in prep

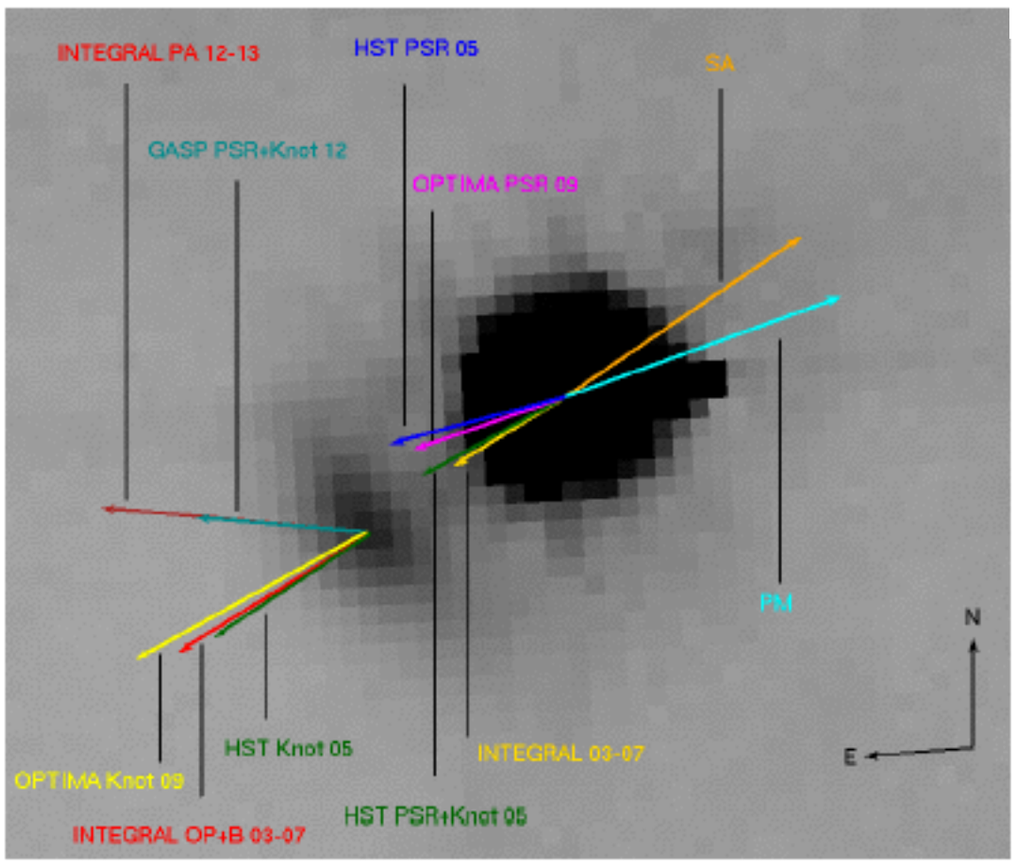

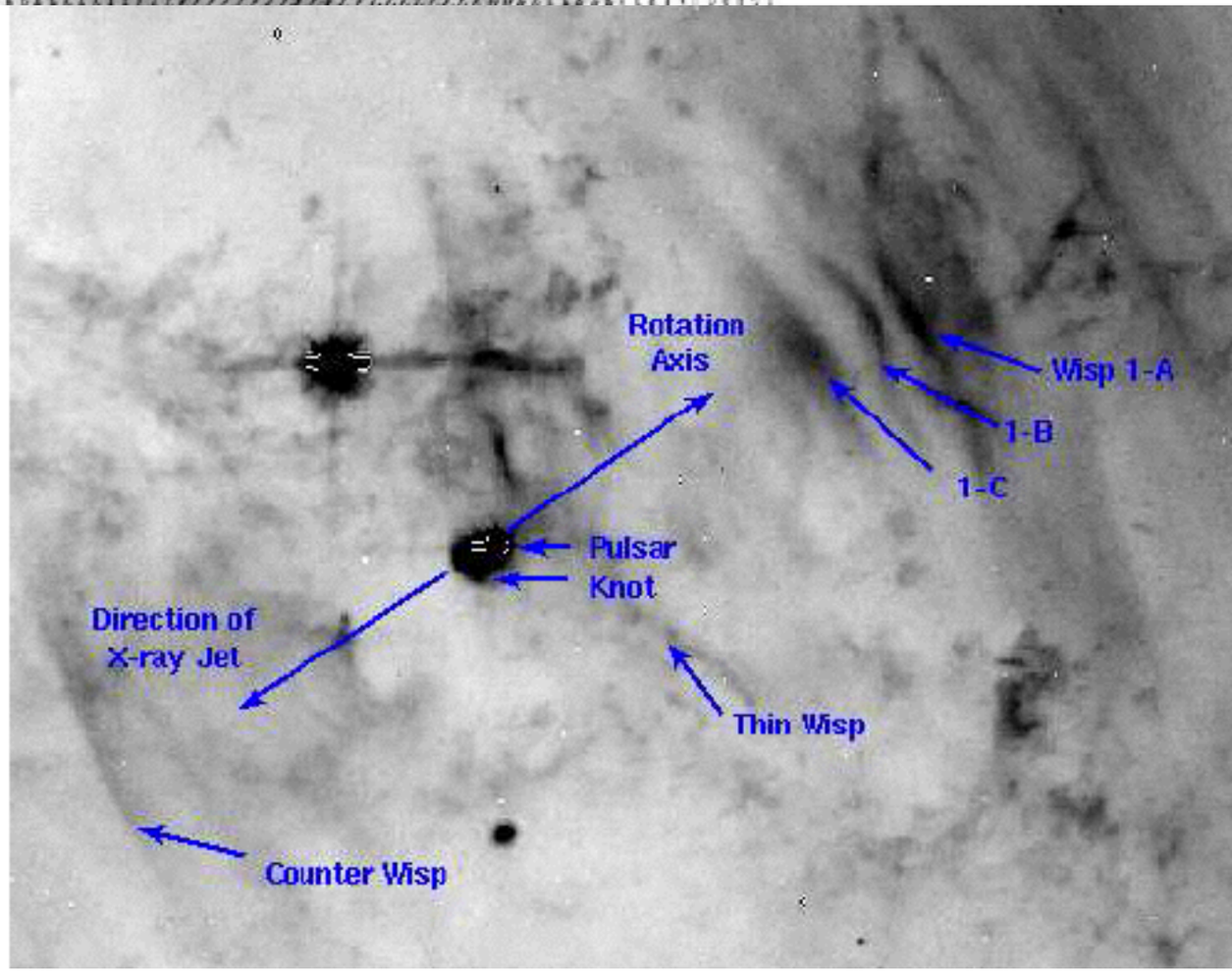

Crab - Optima Observations

Słowikowska et al., 2009, MNRAS.397, 103

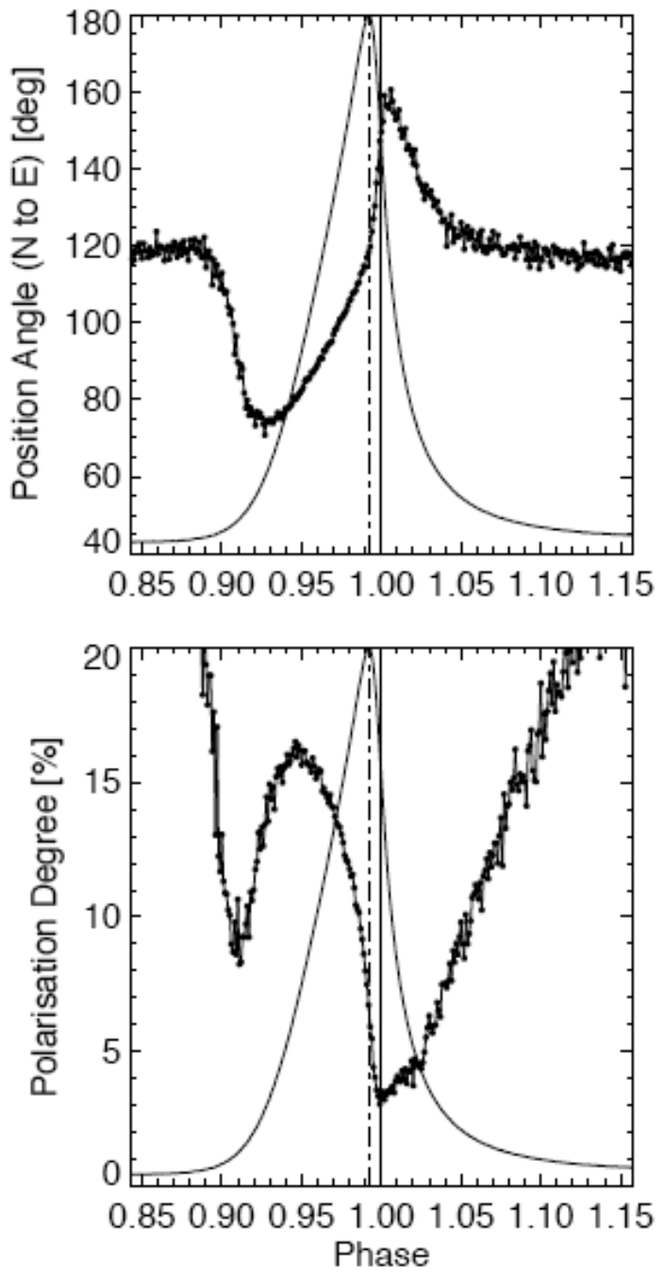

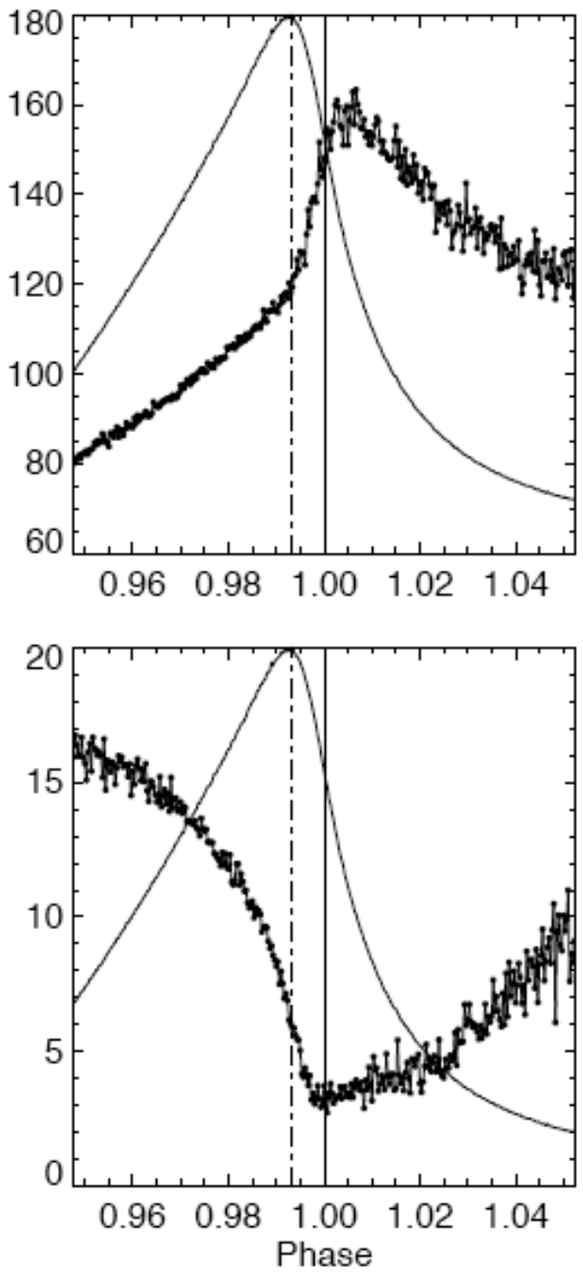

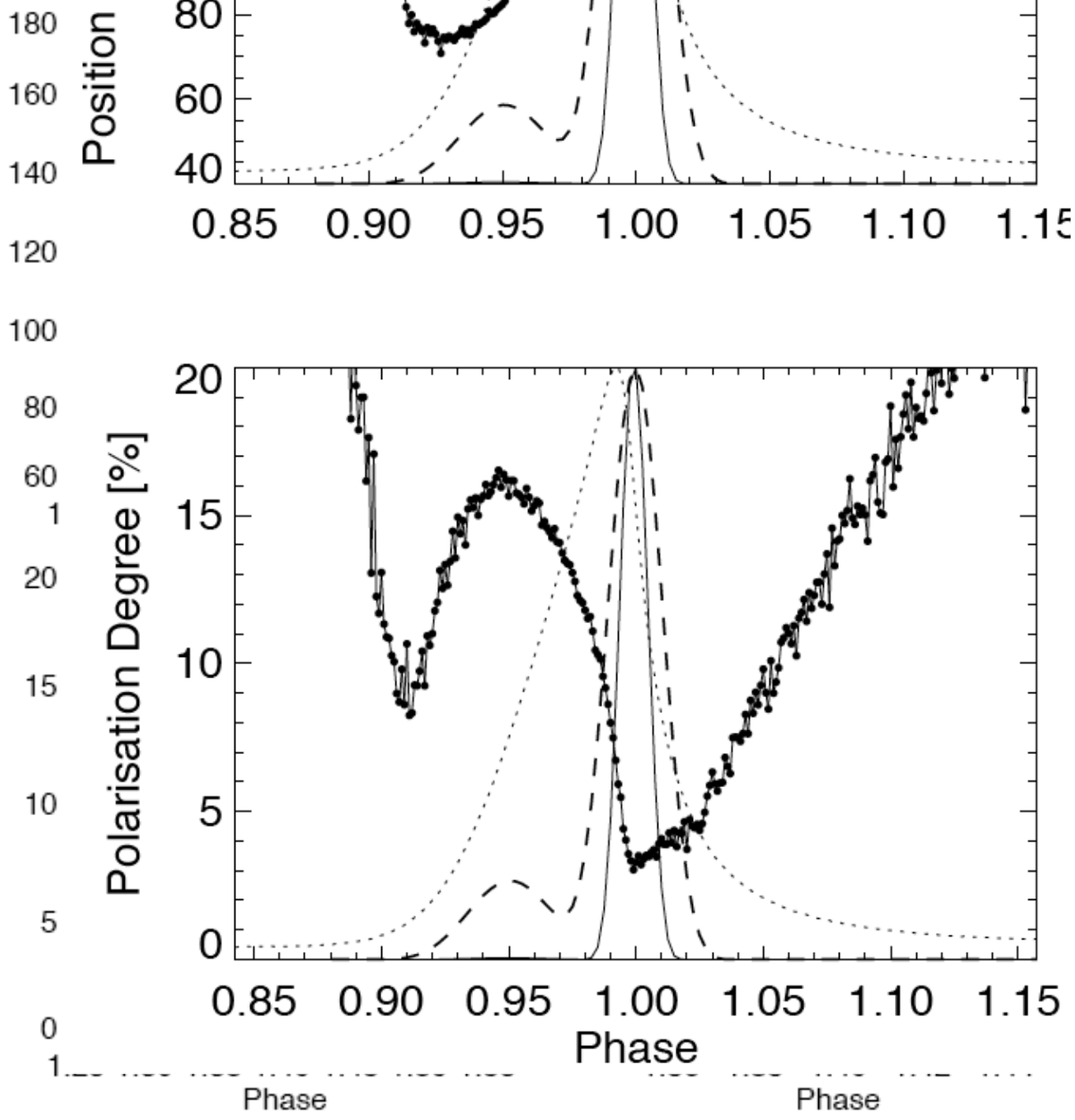

Optical studies and particularly polarisation can separate models - taken from Słowikowska et al 2009

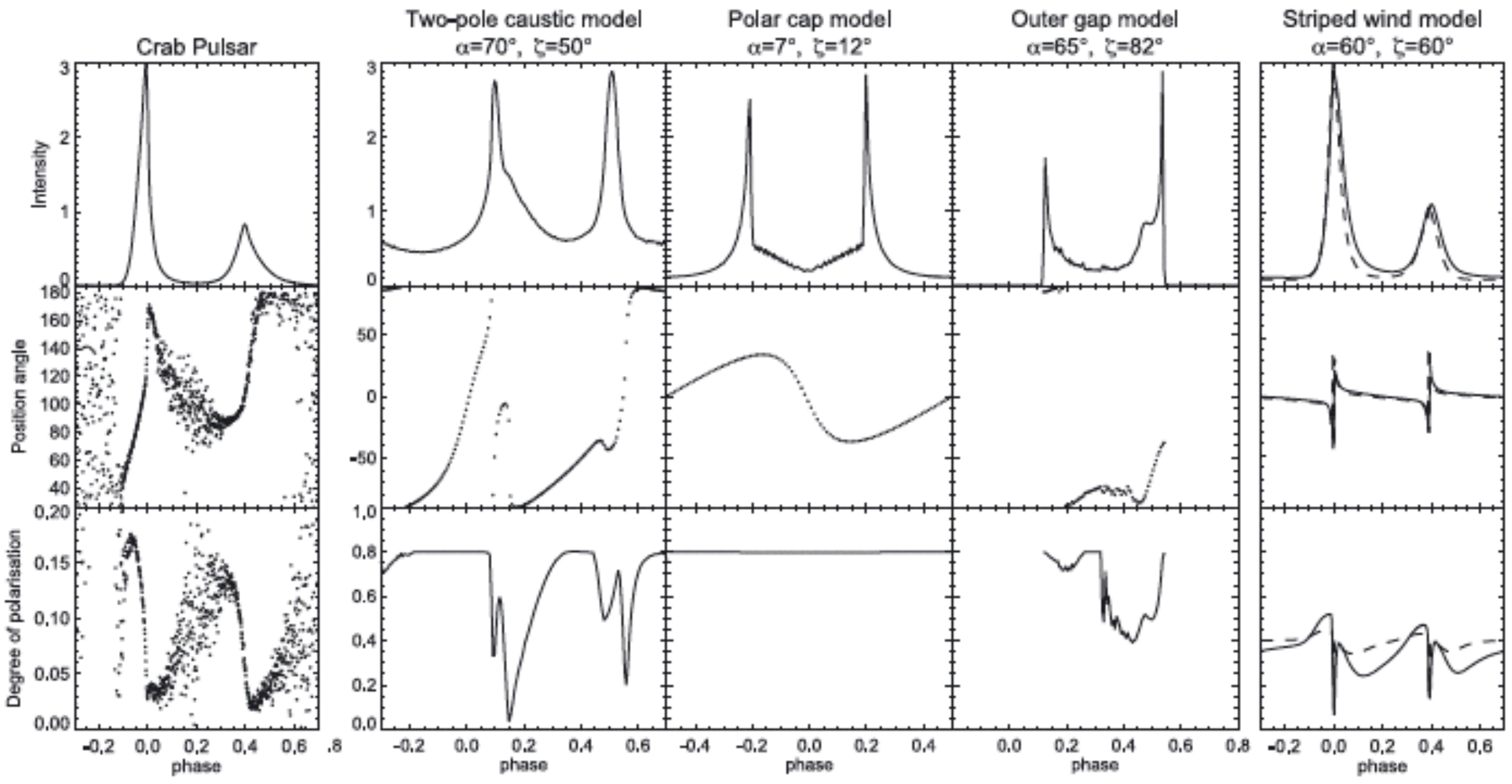

Figure 10. Comparison between observations and models. The left-hand column shows results of our measurements of the Crab pulsar (DC subtracted) opt polarization characteristics, i.e. light curve (Stokes I), PA and PD as a function of pulsar phase (from top to bottom, respectively). In the next four columns, optical light curve, PA and PD calculated for the following high-energy radiation models are shown: the two-pole caustic model; the polar cap model and outer gap model (Dyks et al. 2004b), as well as the striped wind model (Pétri & Kirk 2005). The latter model is calculated for two Lorentz factors, 20 and They are shown as solid and dashed lines, respectively. (We thank to Jarek Dyks and John Kirk for supplying the numerical values.)

Crab - Polarisation

Polarisation studies
Smith et al, 1988, MNRAS, 233, 667
Romani et al, 2001, ApJ
Słowikowska et al., 2009, arXiv:0901.4559v1

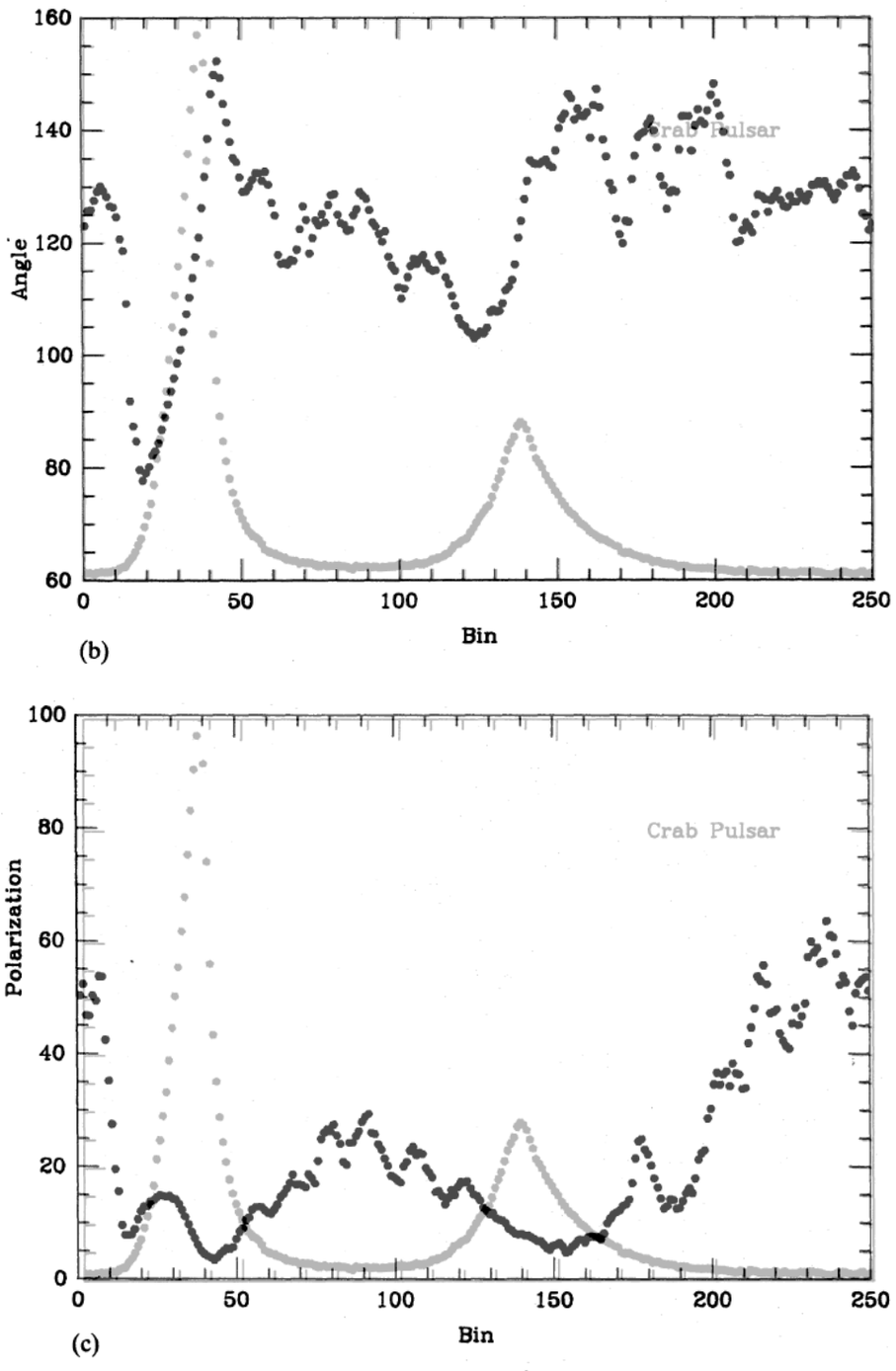

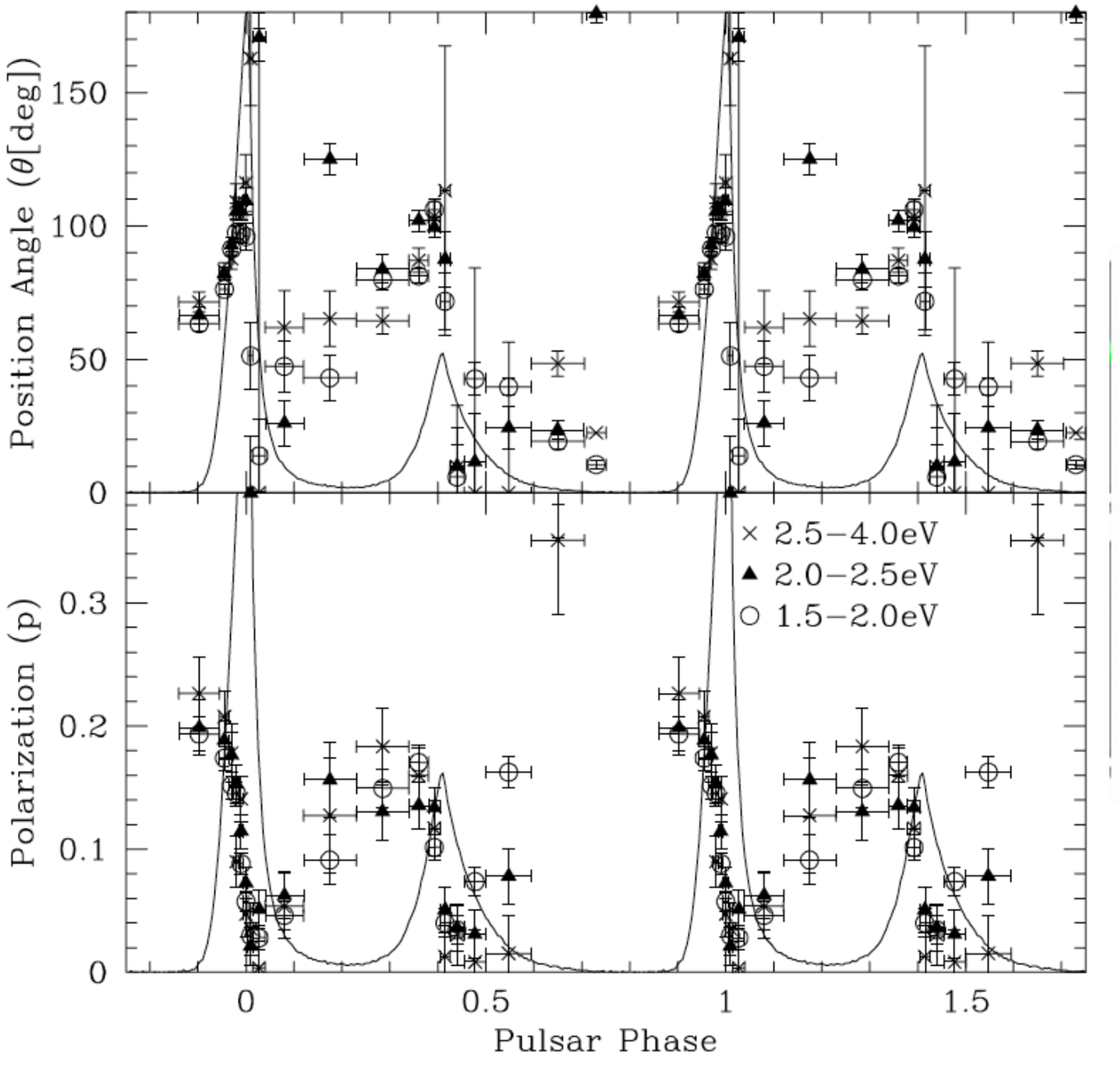

Crab - Polarisation reverse engineering

McDonald et al, 2010, MNRAS

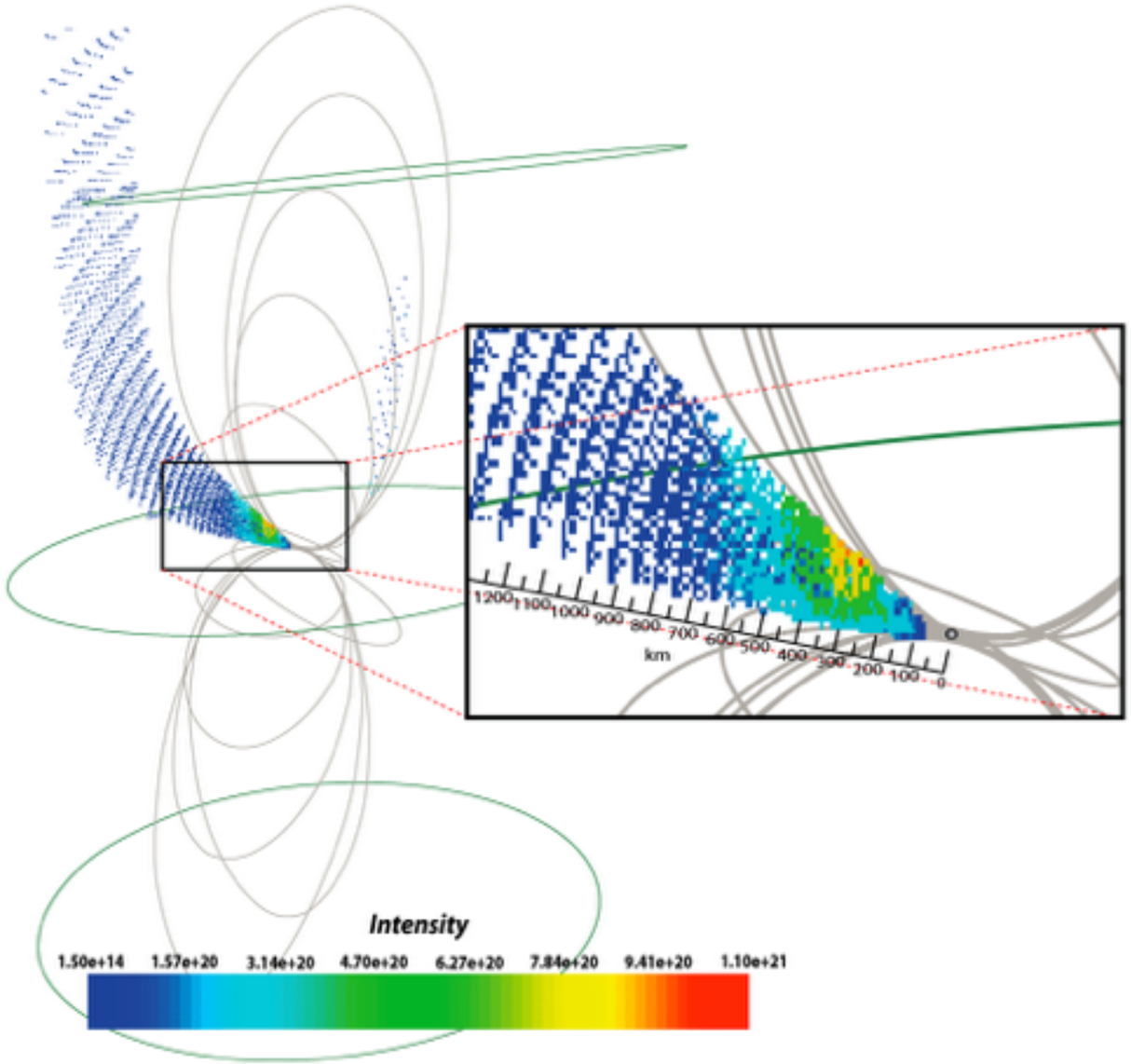

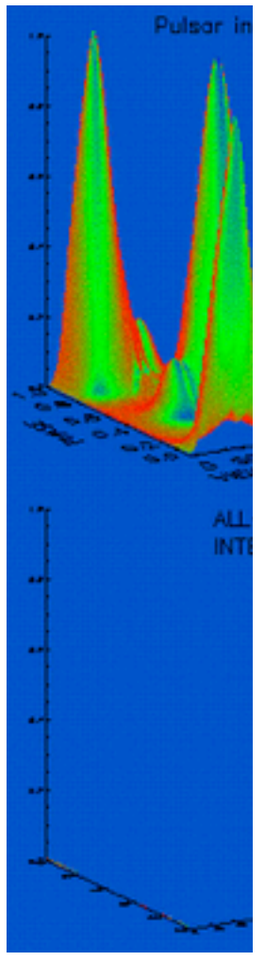

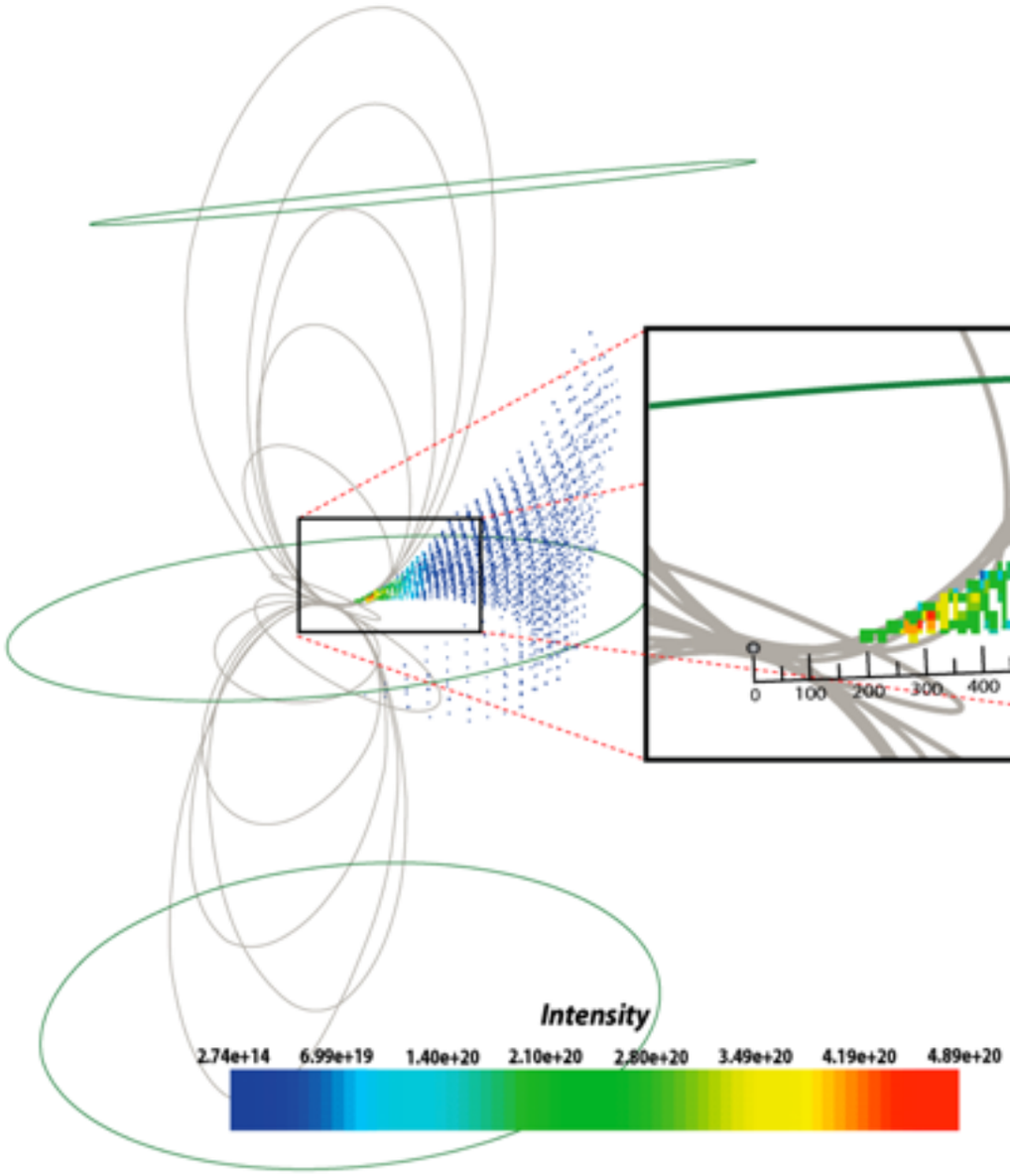

Crab - Optical radio link

255±21μs - Oosterbroek et al
231±68μs - Słowikowska et al

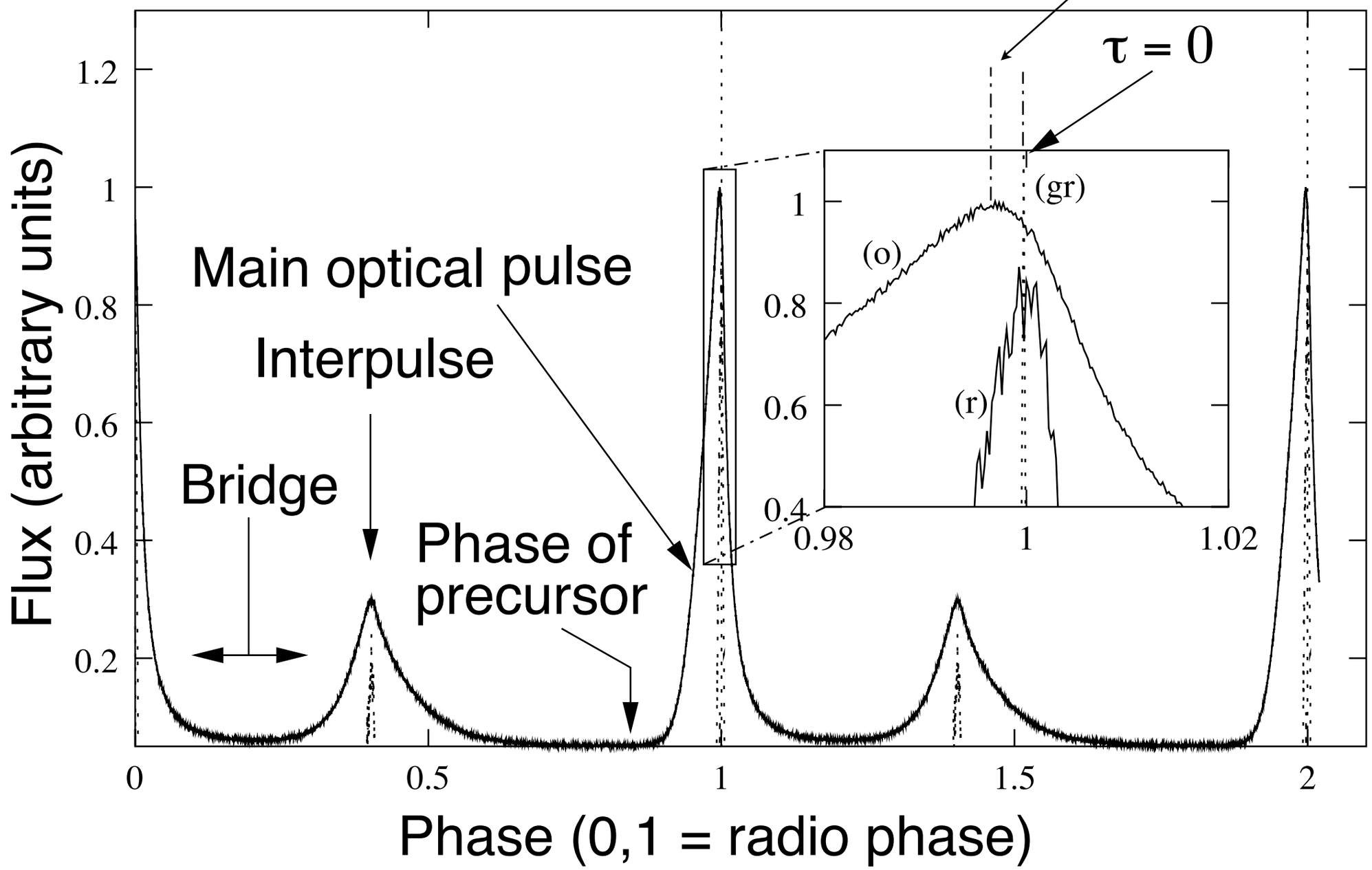

Crab - Optical Radio link - Giant Radio Pulses

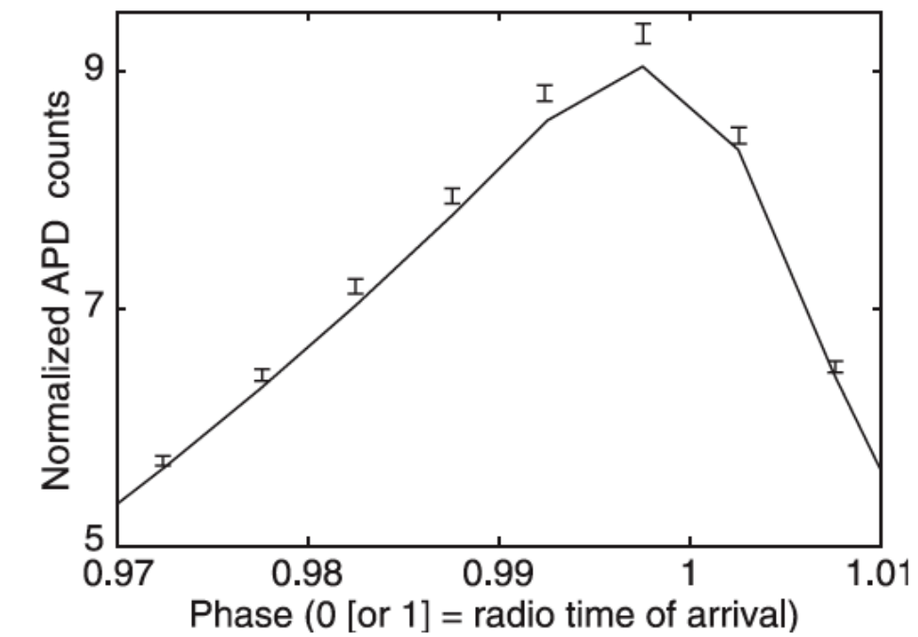

Shearer et al, 2003, Science, 301, 493

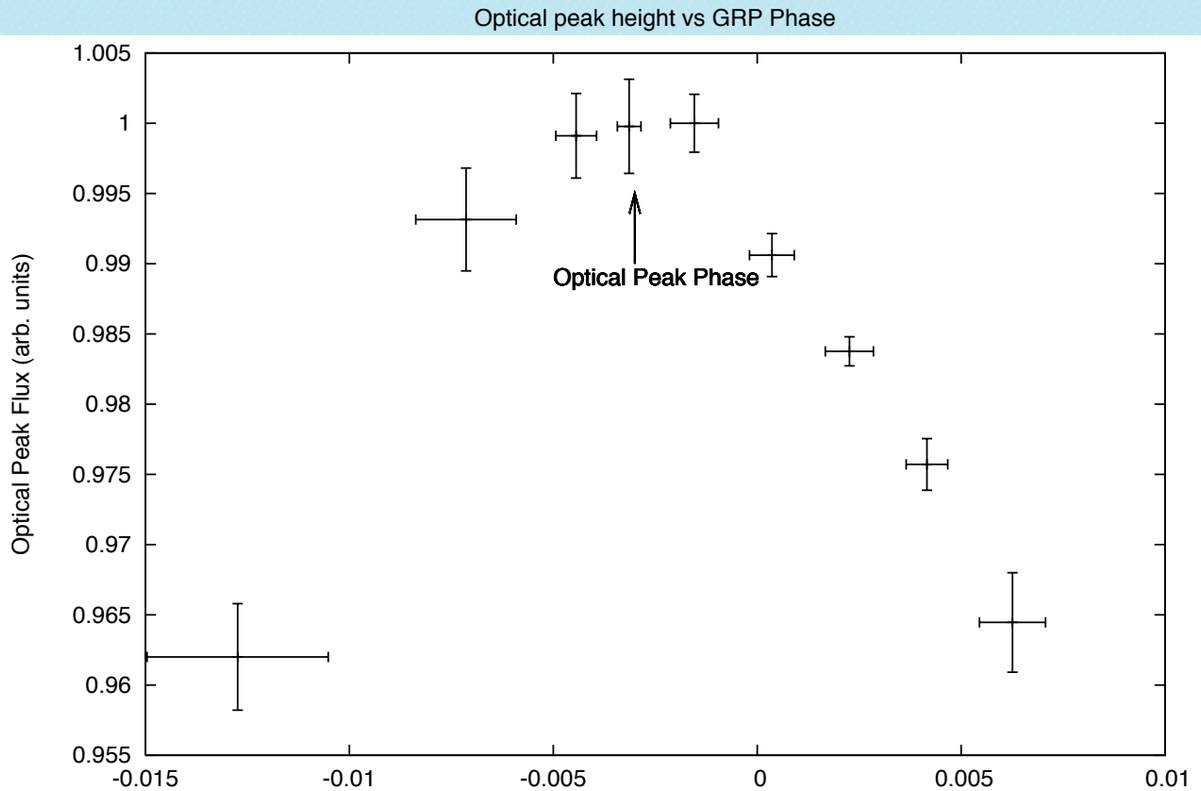

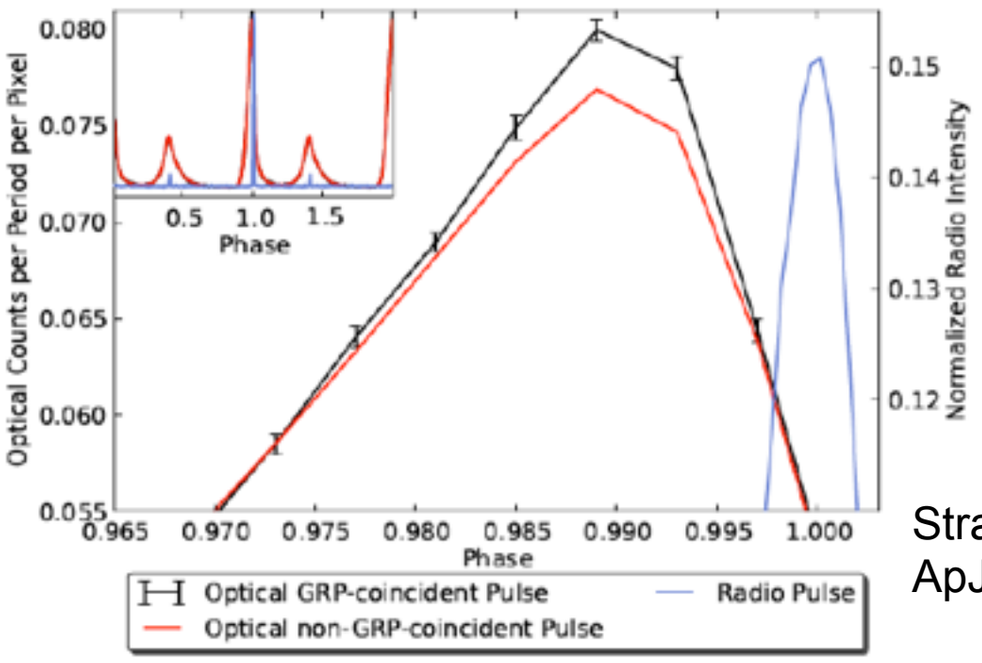

Strader et al, 2013, ApJ, 779, L12

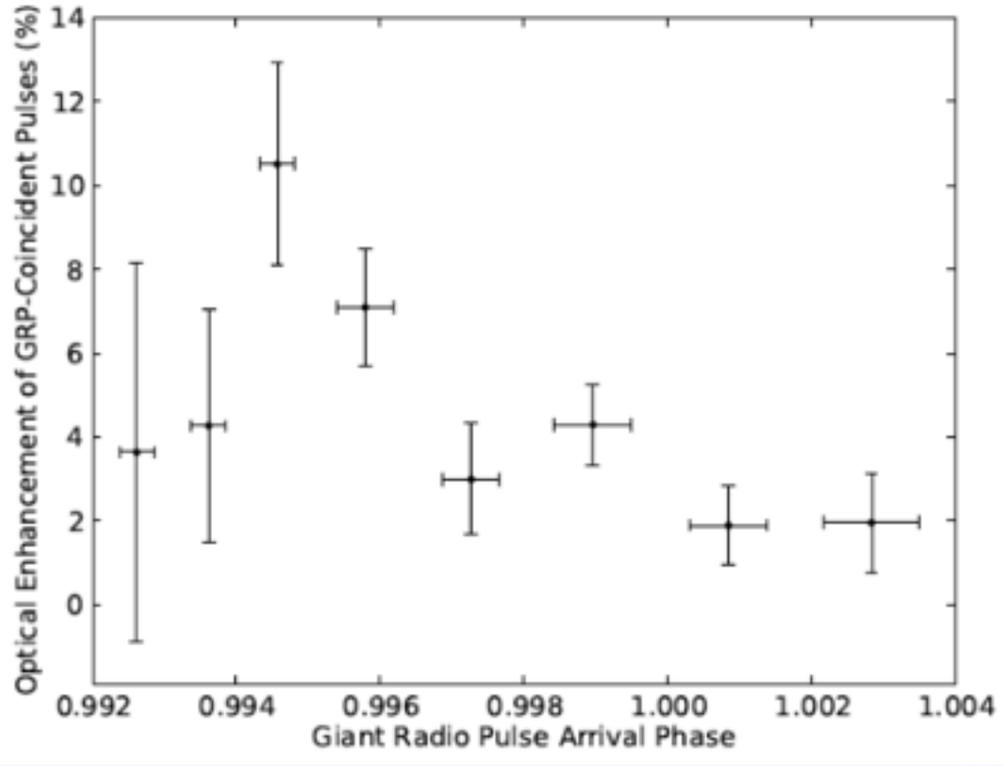

Crab - Optical Radio link - Giant Radio Pulses

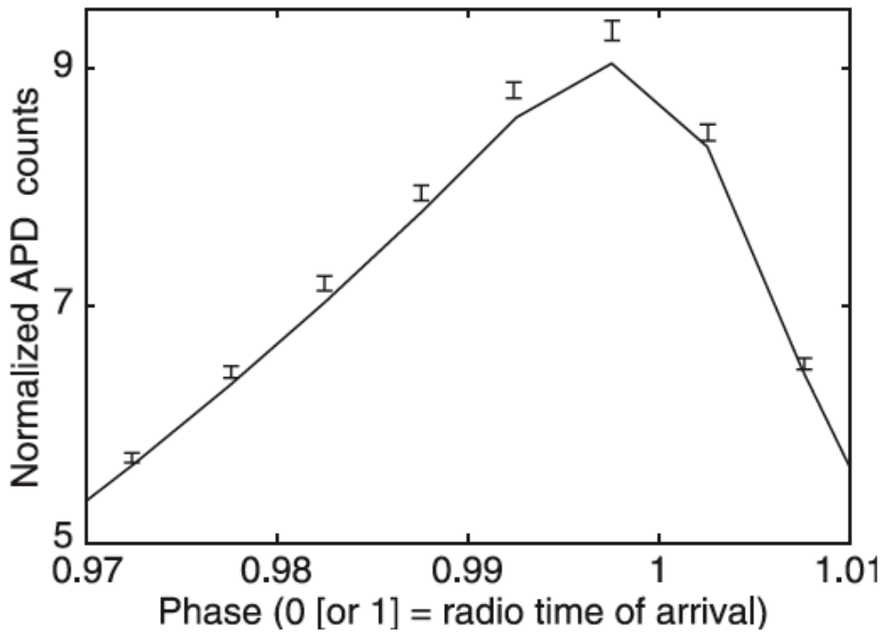

Shearer et al, 2003, Science, 301, 493

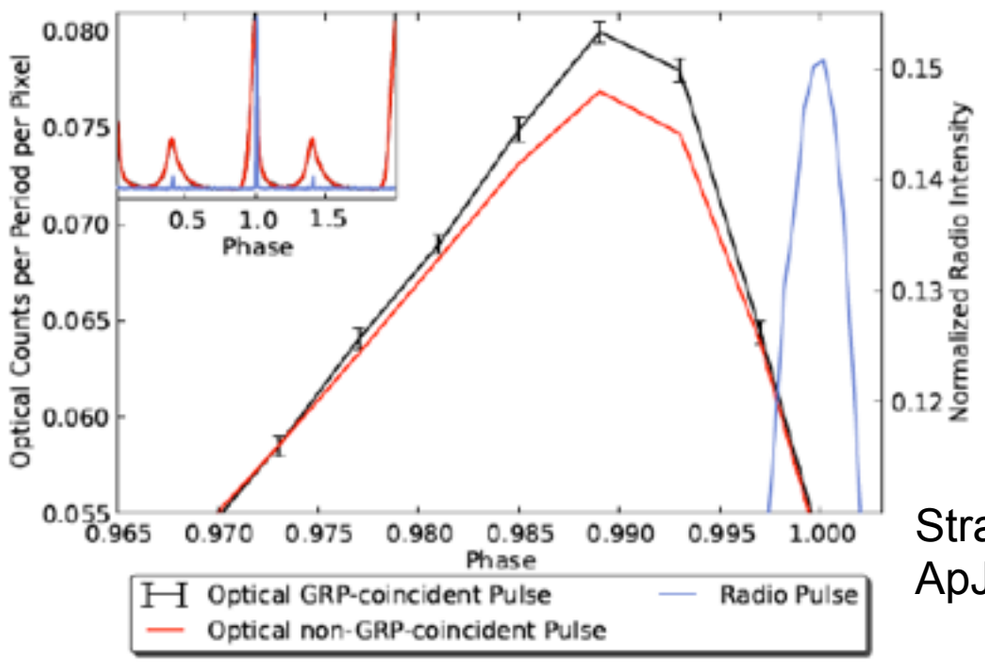

Strader et al, 2013, ApJ, 779, L12

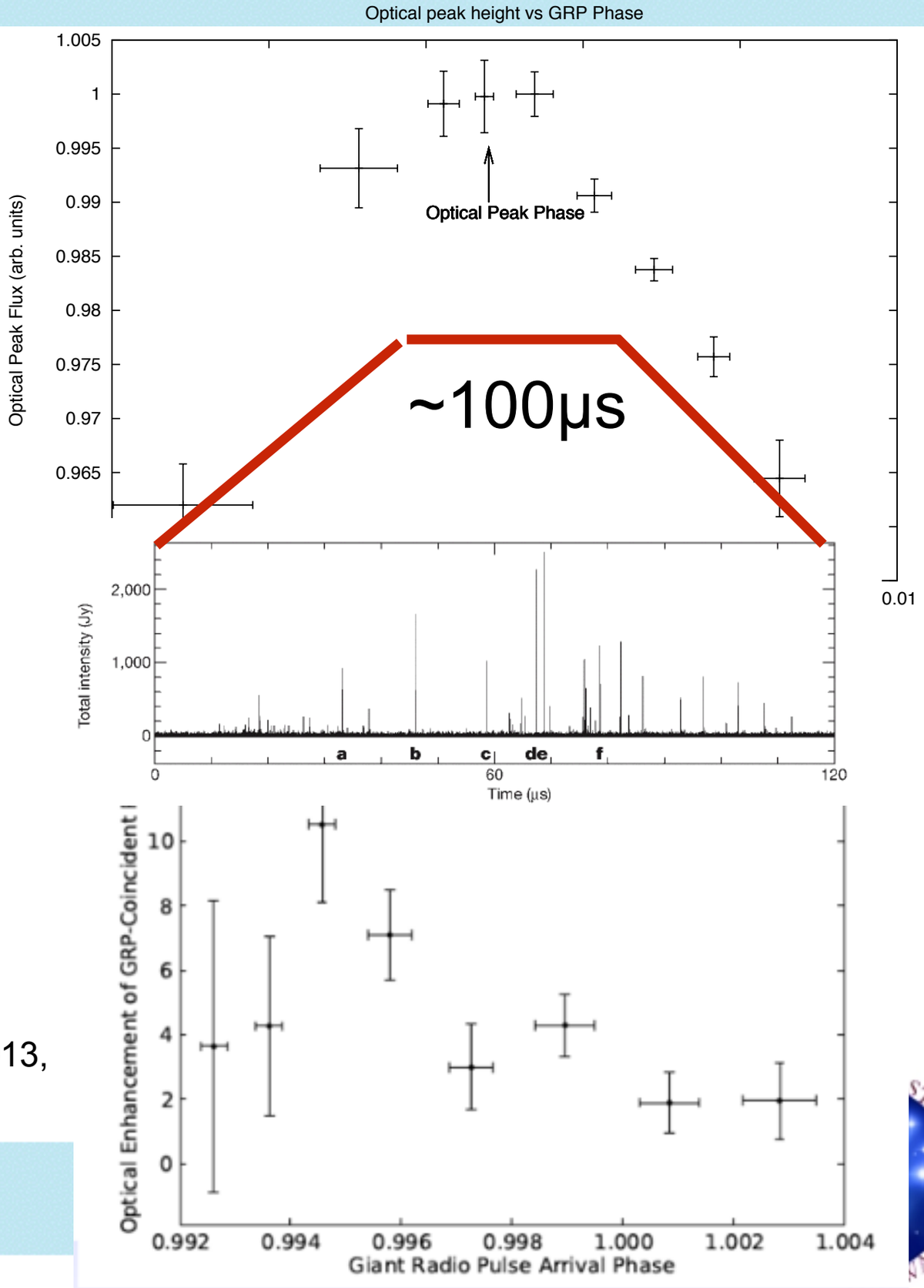

Crab - rising edge

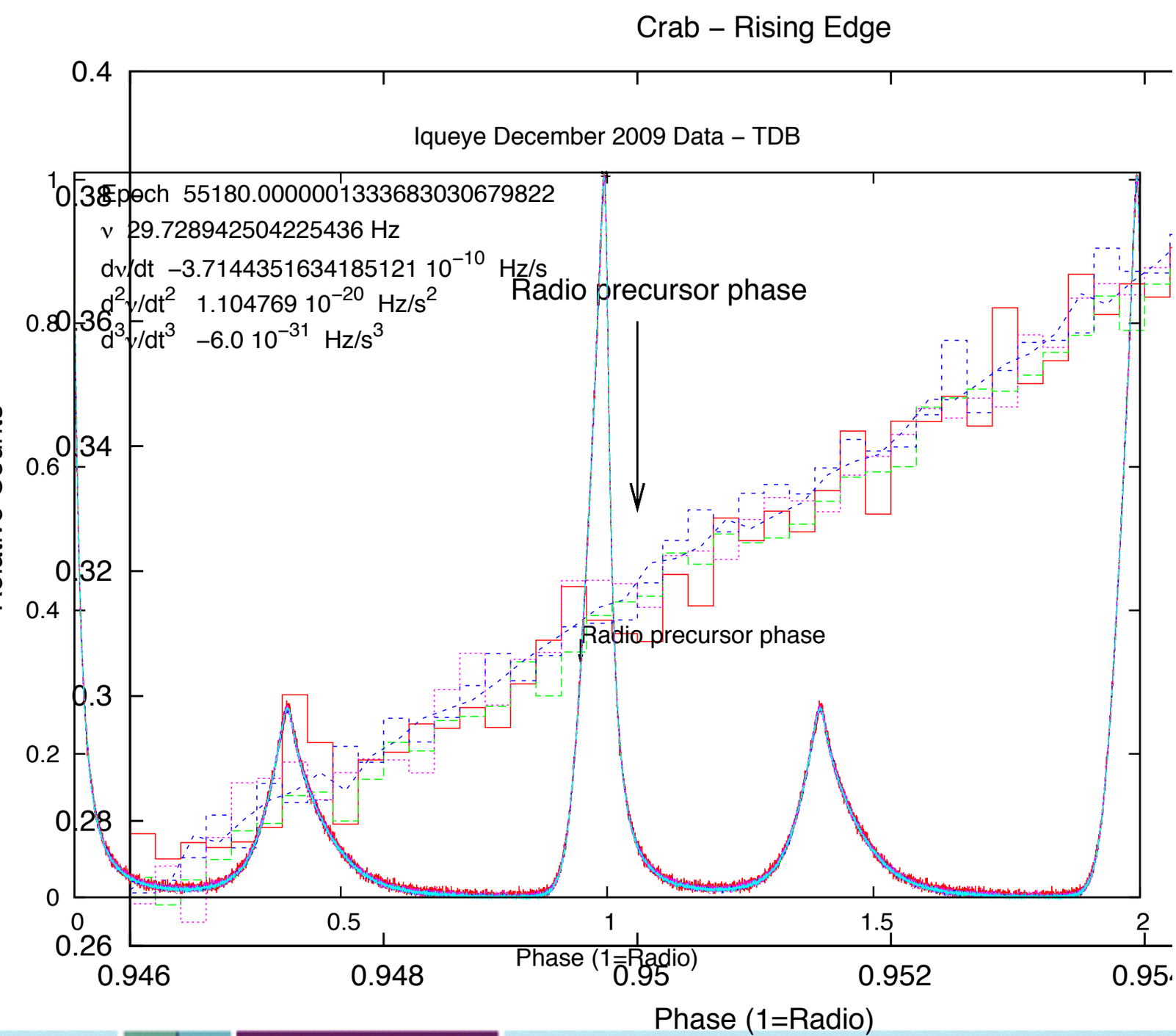

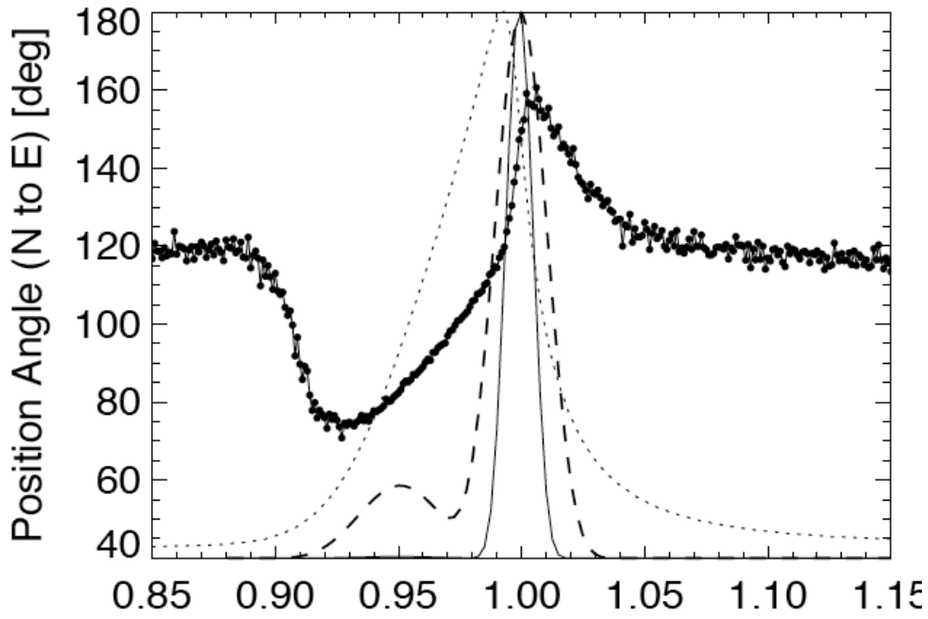

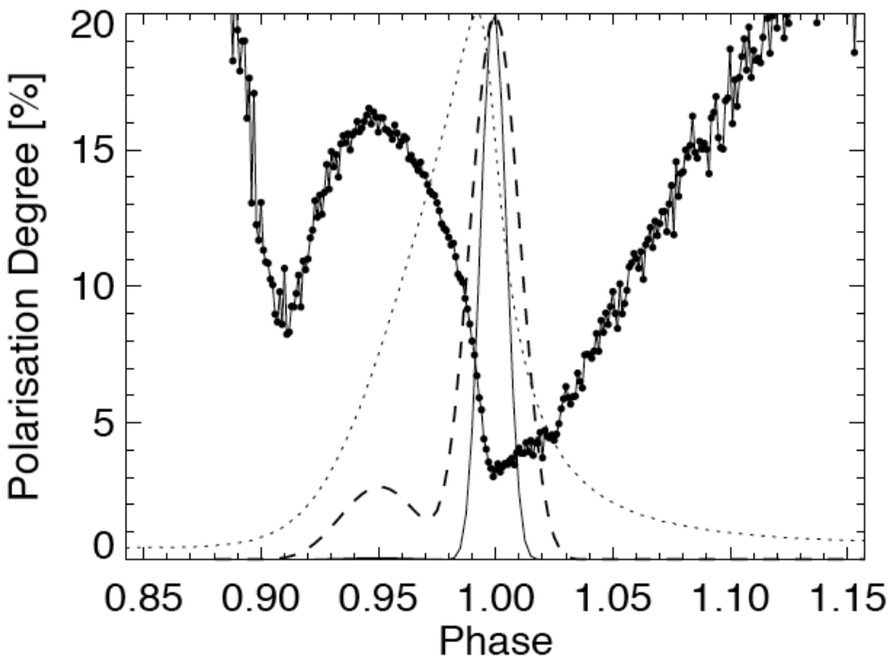

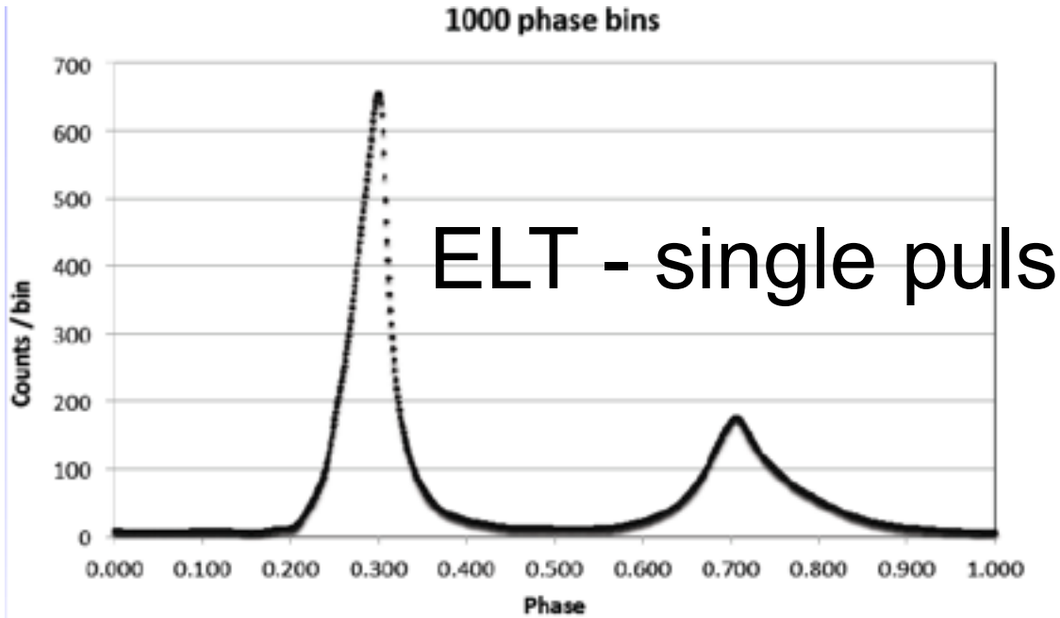

ELT - single pulse

Stochastic variability?

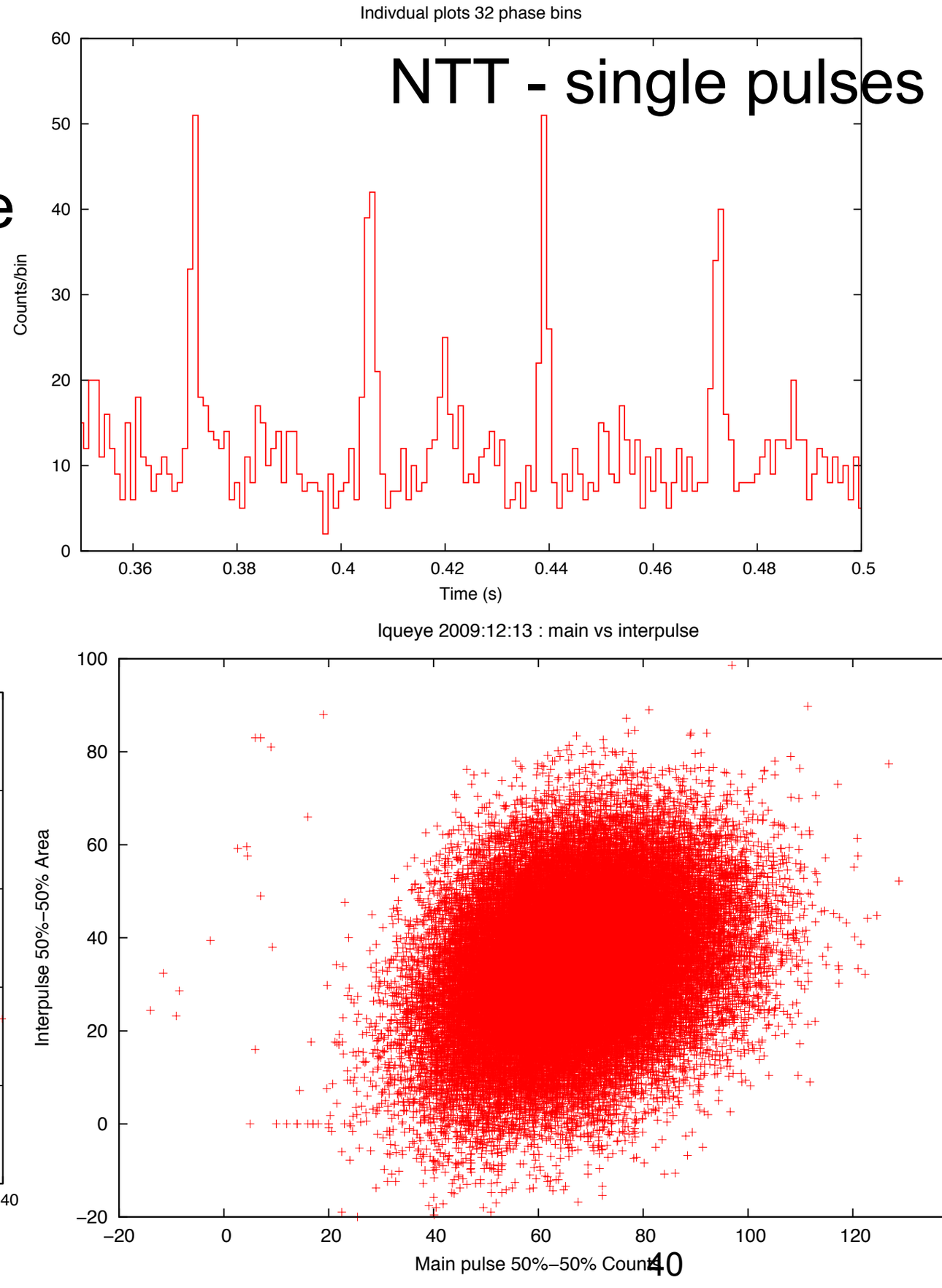

NTT - single pulses

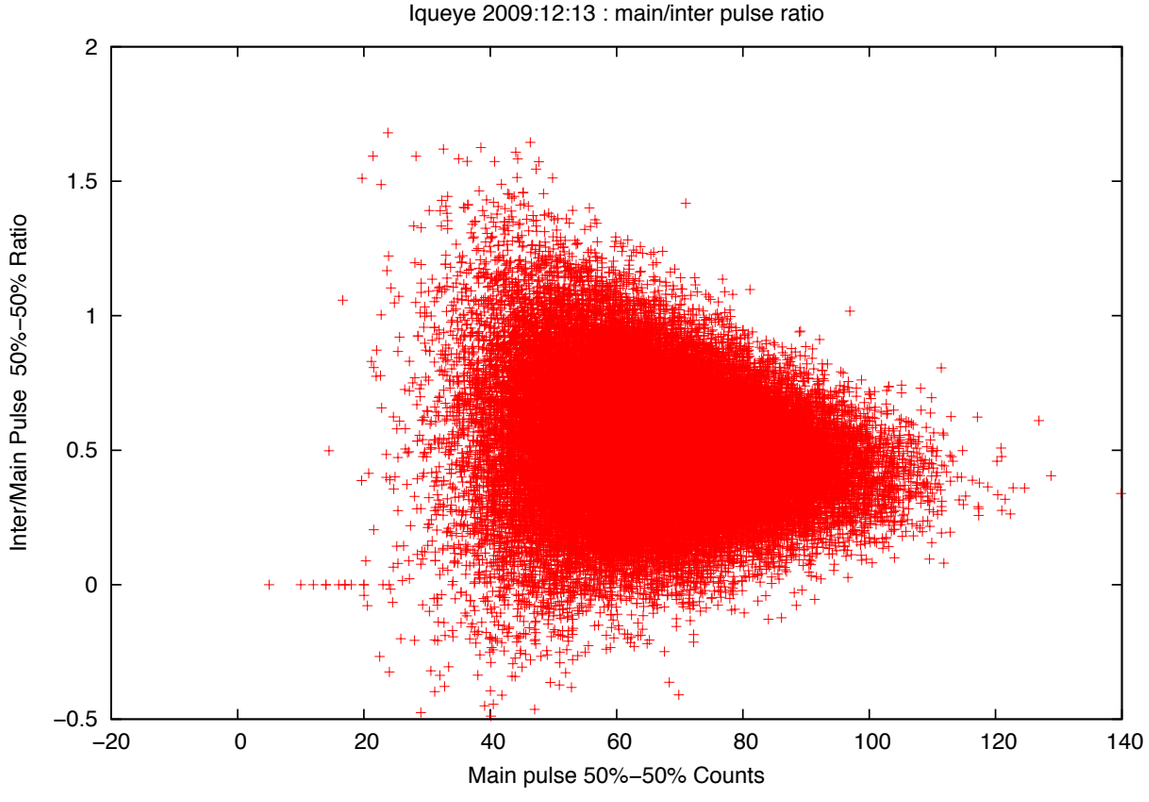

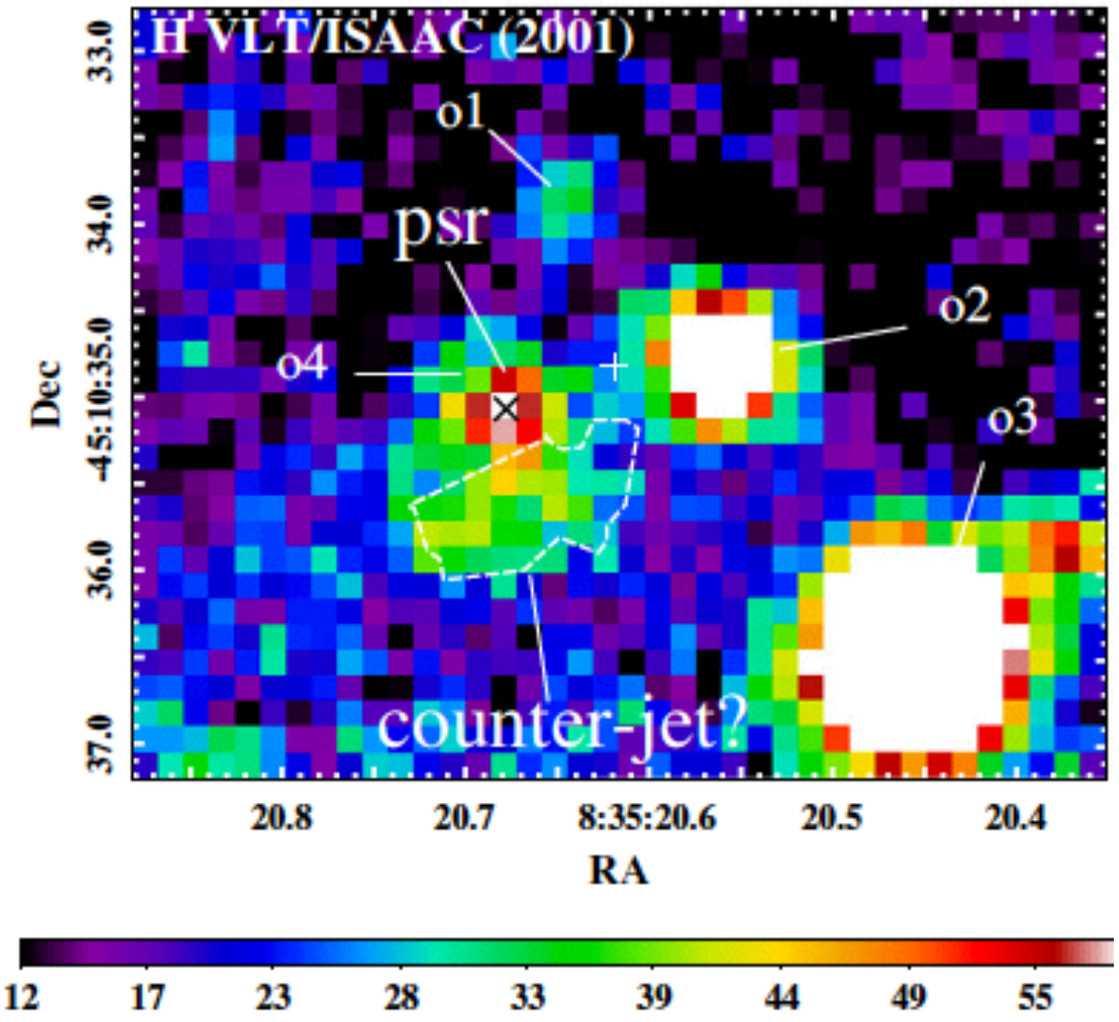

Figure 1. 5.″5 × 4.″5 fragment of the Vela pulsar vicinity as seen with the VI
and nearby field objects are marked using notations from Shibanov et al. (2(
seven-pixel Gaussian kernel to better underline the morphology of the exten
in the right frame indicates the projection of the X-ray counter-jet axis on t
and Gemini (2013) observations, respectively. The long and short arrows ind
extended feature, respectively. The polygon is the aperture used for the phot

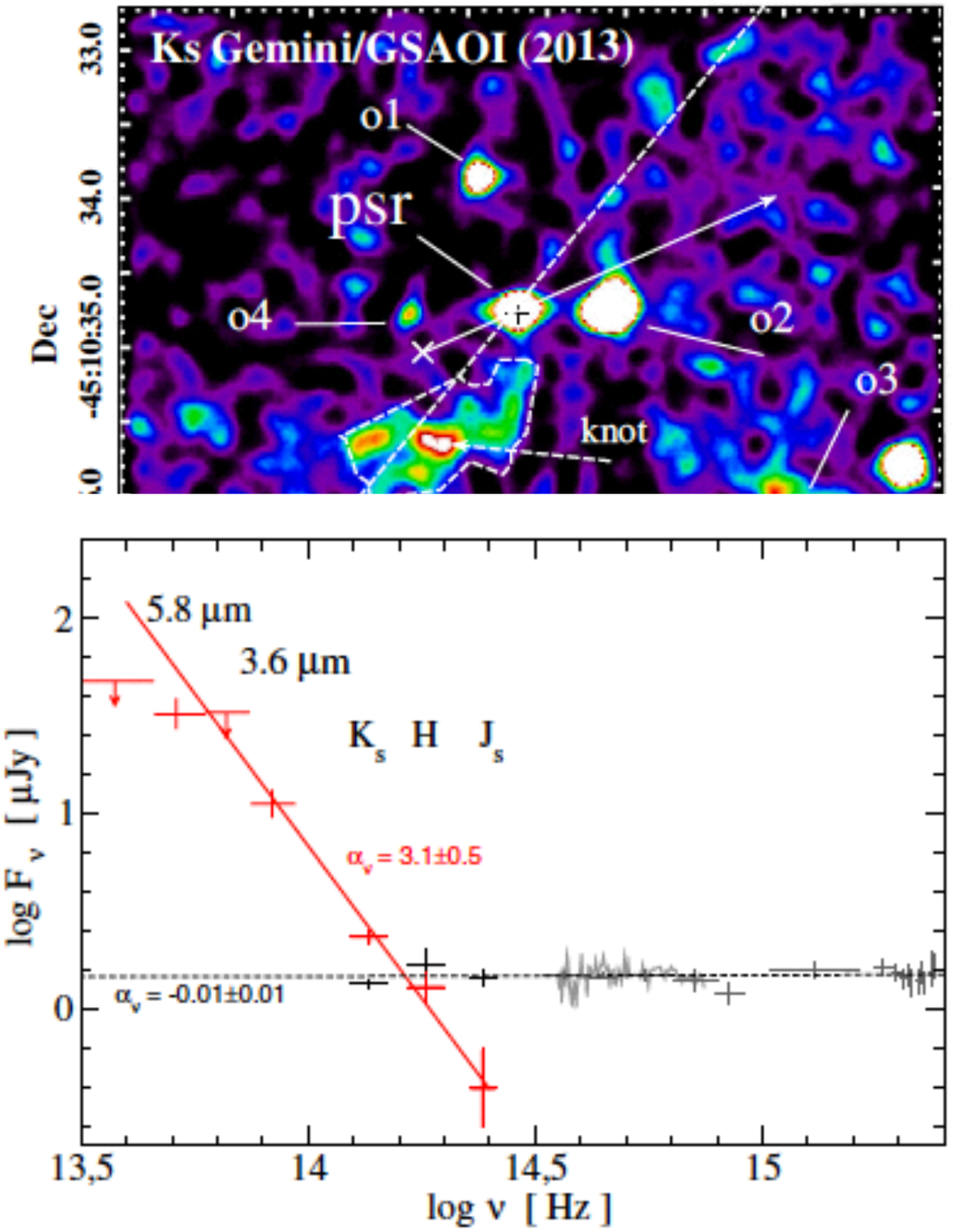

Figure 2. IR–UV spectra of the Vela pulsar (black/gray) and the likely counter-jet feature (red). The UV–optical data are from Romani et al. (2005) and Mignani et al. (2007) and the IR data are from Shibanov et al. (2003) and Danilenko et al. (2011). The dashed line approximates the flat UV–optical spectrum of the pulsar. The red line is the best fit to the near-IR fluxes of the counter-jet. The index α_ν is defined as $F_\nu \propto \nu^{-\alpha_\nu}$.

Vela : K Band

NUI Galway
OÉ Gaillimh

ETTORE MAJORANA FOUN
CENTRE FOR SCIENTIFIC

Optical/NIR Magnetars
4U 01642+61 : Wang et al, 2006, Nature, 440, 772

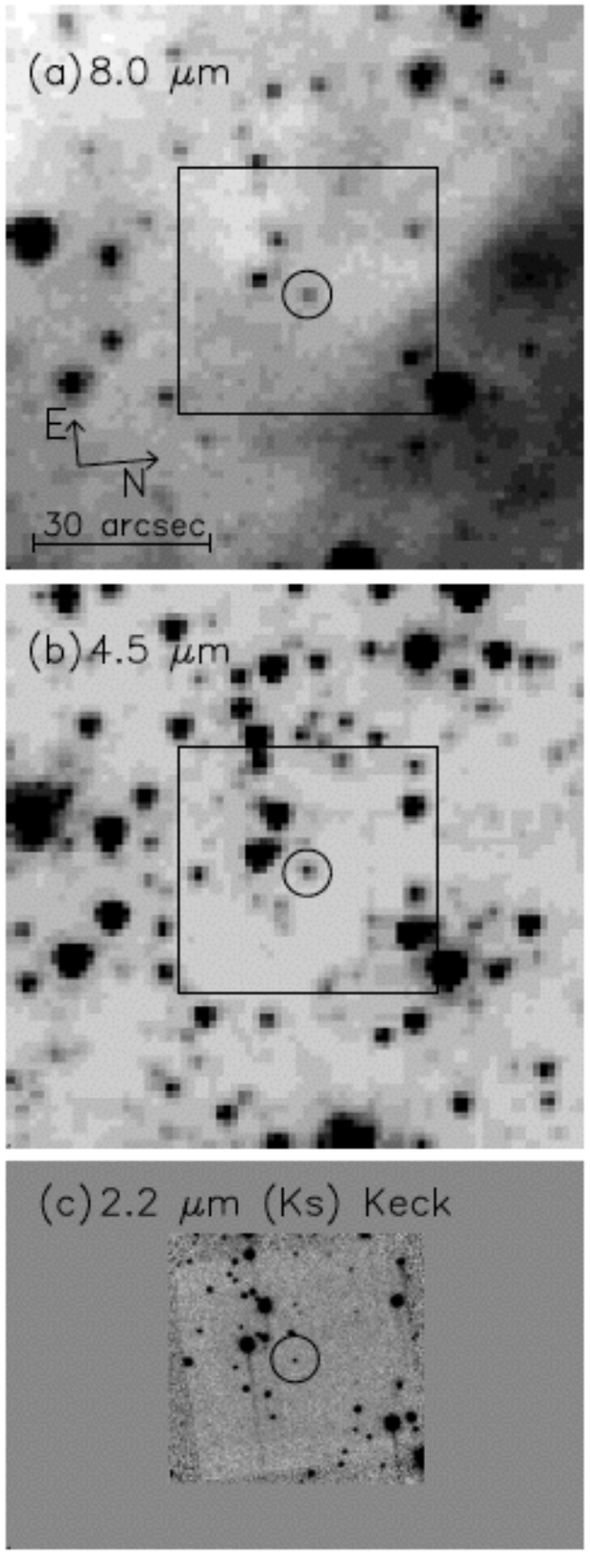

SGR1806-20	2004	3.14	20.1	15	29	IR
1E 1547.0-5408	2009	3.14	18.5	9	17	IR
1E 1048.1-5937	2004	3.63	21.3	3	6.1	OIR
XTE J1810-197	2004	3.75	20.8	4	5.1	IR
SGR 0501+4516	2009	4.1	19.1	~2	5	IR
4U 0142+61	2002	4.84	20.1	>5	5.1	OIR
1E 2259+586	2002	5.34	21.7	3	5.7	IR

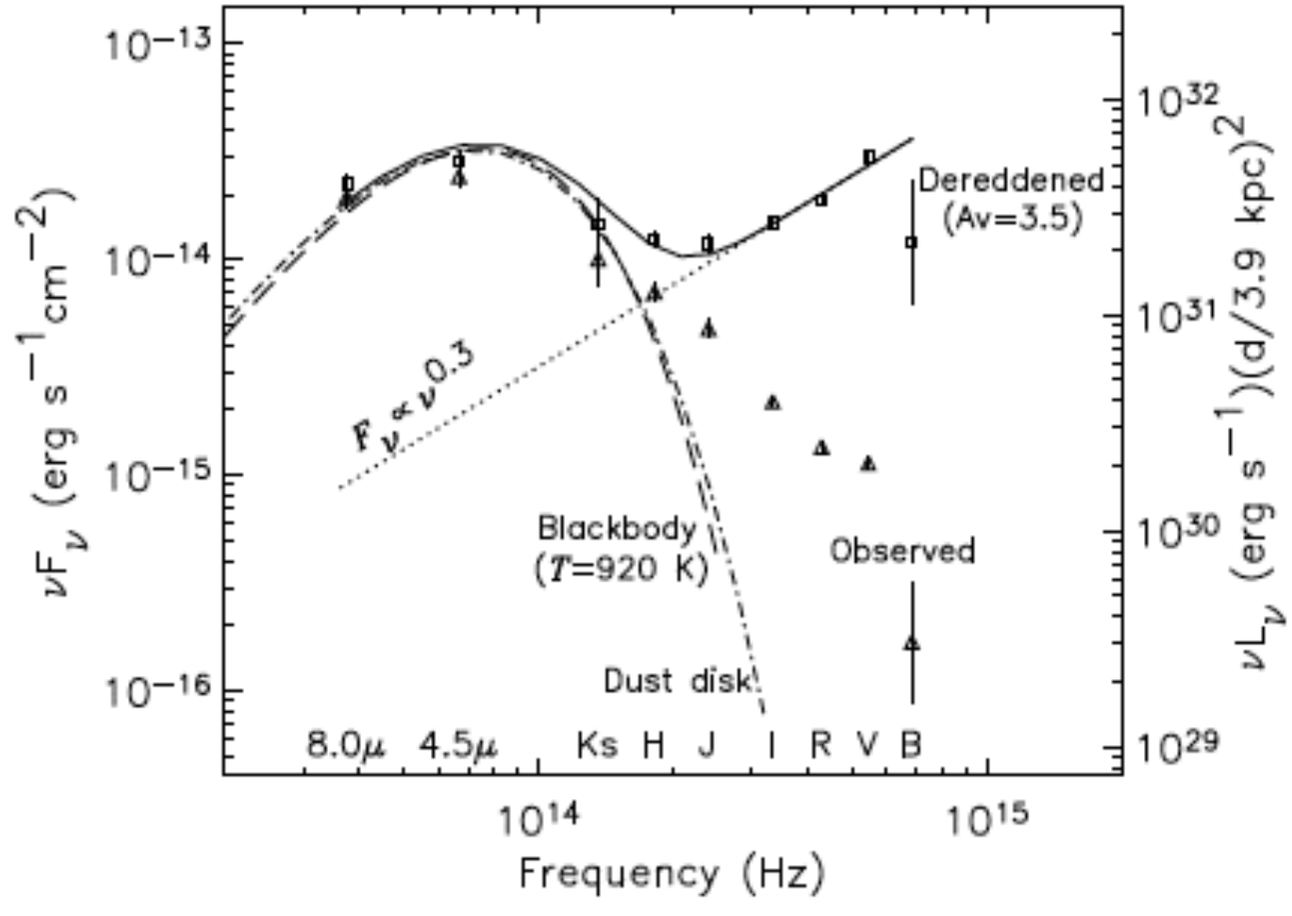

4U01642+61 : Dhillon et al, 2006, 363, 609

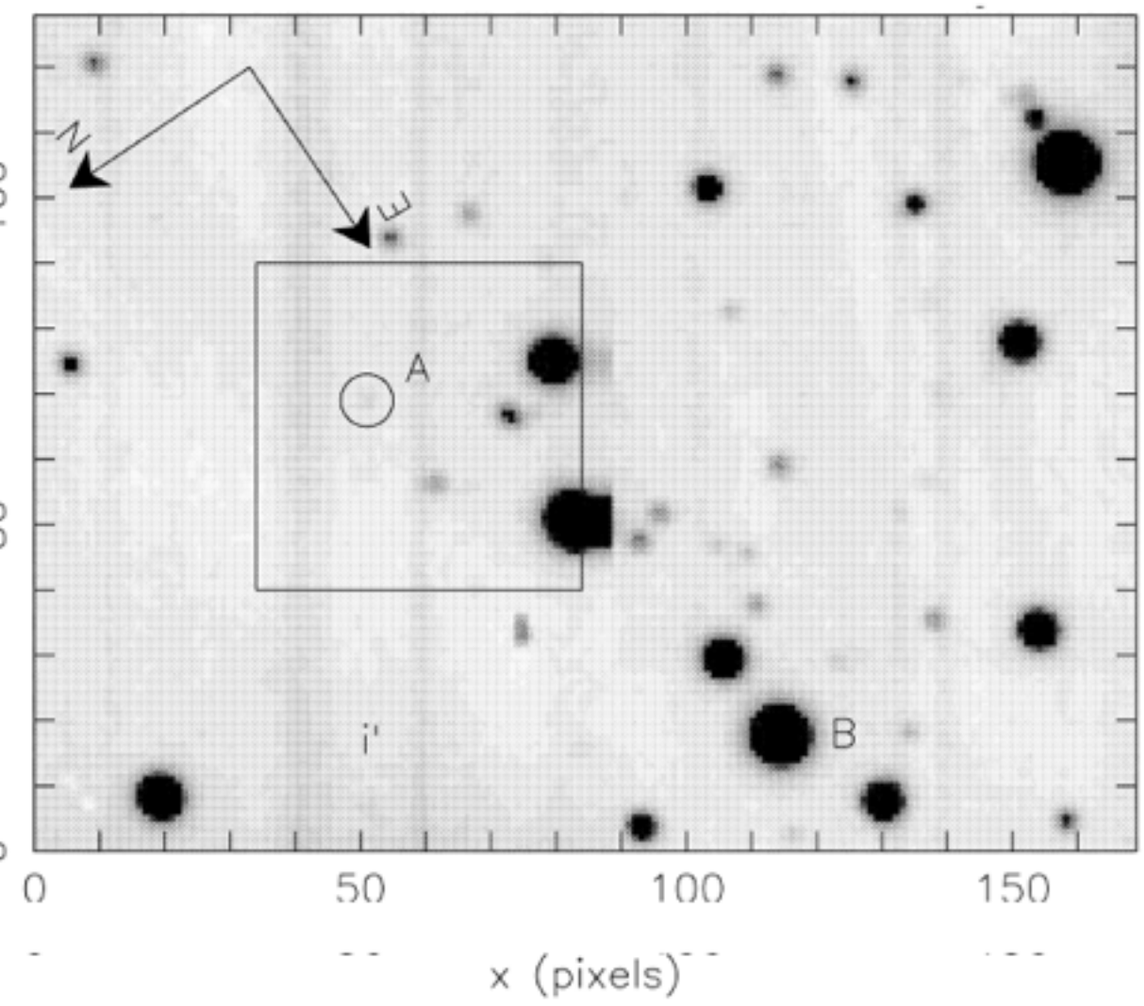

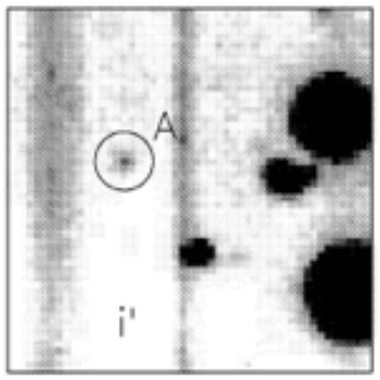

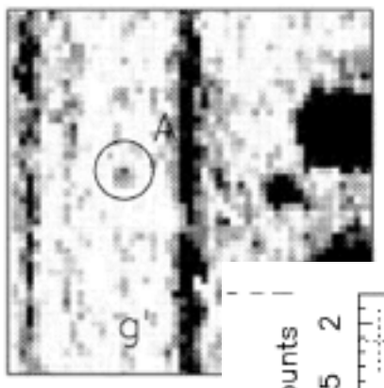

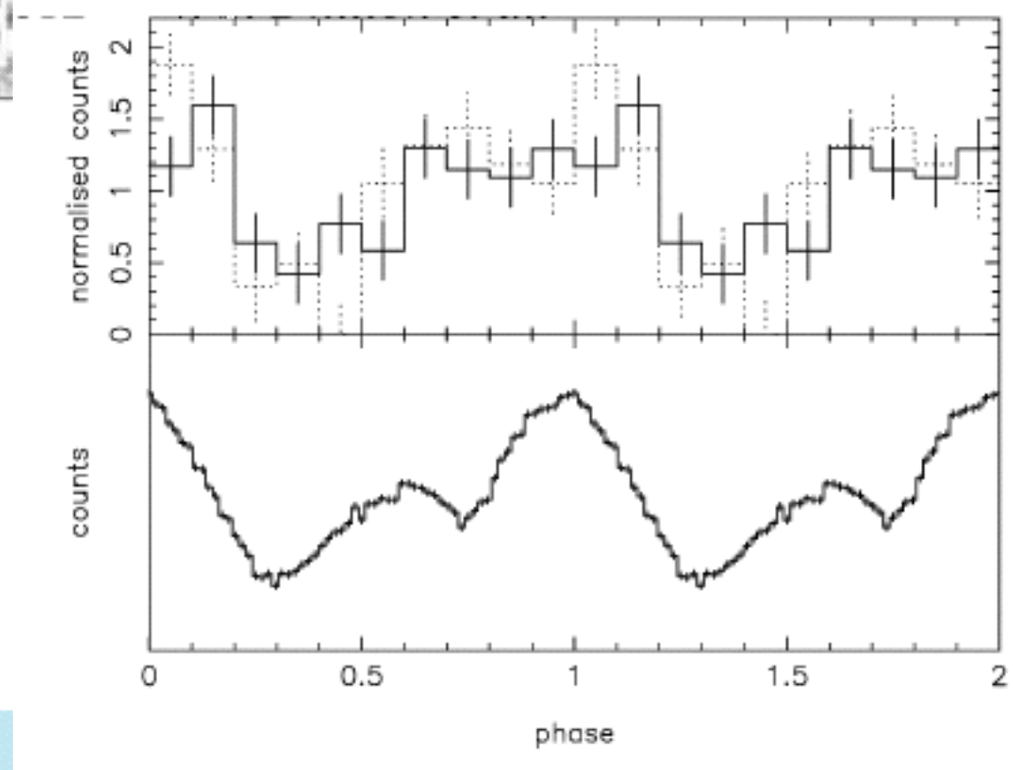

Figure 2. Top: pulse profiles of 4U 0142+61 in the i' band on 2002 September 12 (solid line), obtained using technique (i) (Section 2.1). The dotted line shows the poorer-quality light curve we obtained on the night

NUI Galway
OÉ Gaillimh

ETTORE MAJORANA FOUNDATION AND CENTRE FOR SCIENTIFIC CULTURE

HTRA Science Case II
Close Binary Systems

X-ray-Optical cross-correlations observed by UltraCam and Optima

Shown are UltraCam observations of the black-hole accretor GX339-4 - Gandhi et al (2008)

Time scales < 1 sec
Optical Autocorrelation indicated synchrotron emission from a possible jet structure rather than being driven by X-ray reprocessing.

GX339-4 is reasonably bright V~17. Other objects considerably fainter - E-ELT required to look at spectral variability

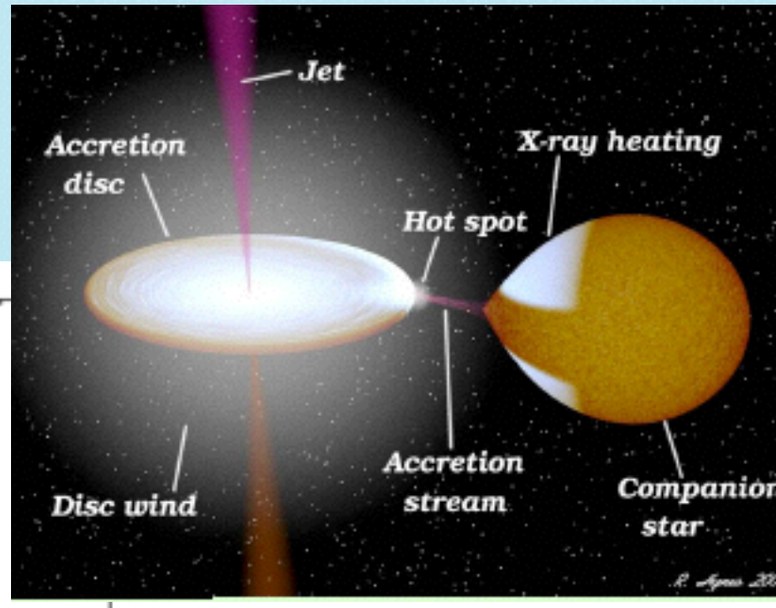

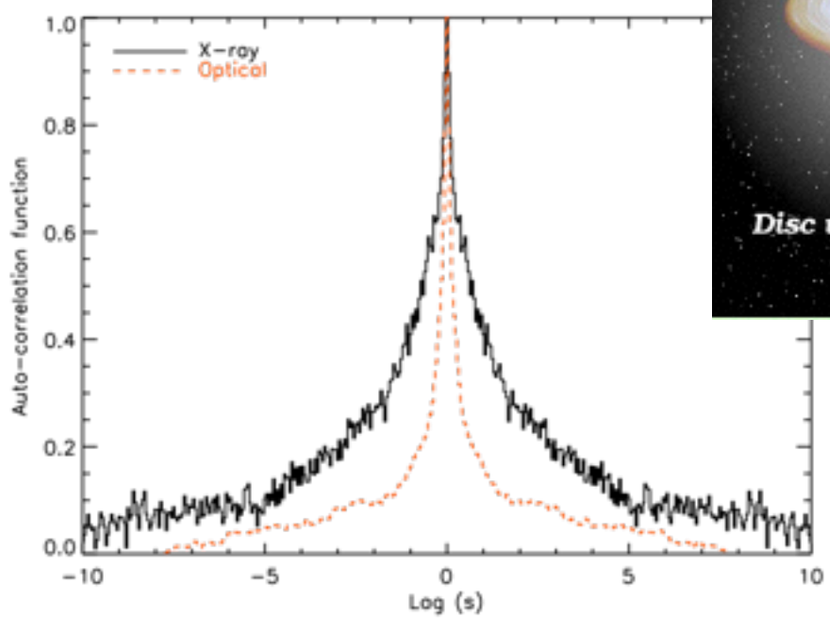

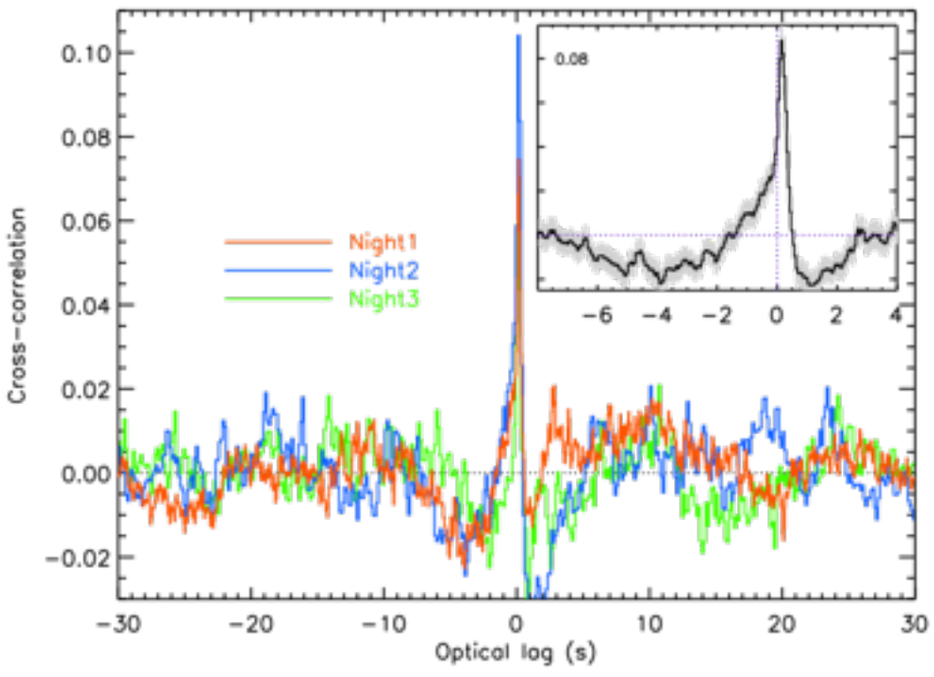

Casella et al, 2020,MNRAS, 404, L21 - RXTE + ISAAC : GX 339-4

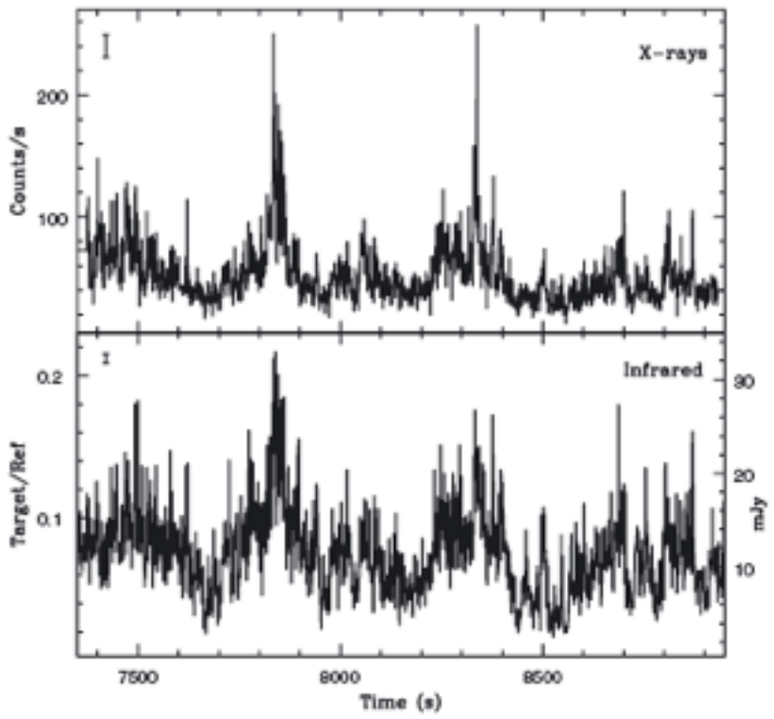

Figure 1. Top panel: a sample of the X-ray light curve of GX 339−4, obtained with the PCA onboard *RXTE*. The data are background subtracted, in the 2–15 keV energy range, at 1-s time resolution. Bottom panel: the simultaneous IR light curve, obtained with ISAAC. We show the ratio of the source (average 4.4×10^5 counts s^{-1}) to the reference-star (6×10^6 counts s^{-1}) count rates in the K_S filter, at 1-s time resolution. The right ordinates show the dereddened flux. We show the typical error bars in the top left-hand corner of each panel.

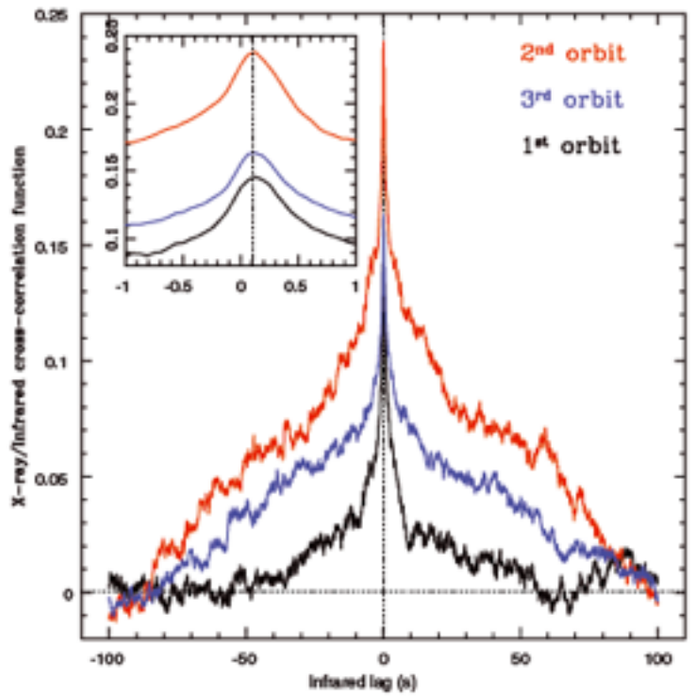

Figure 2. Cross-correlations of the X-ray and IR light curves of GX 339−4 (positive lags mean IR lags the X-rays). A strong, nearly symmetric correlation is evident in all the three time intervals, corresponding to different *RXTE* orbits. In the inset, we show a zoom of the peaks, showing the IR delay of ∼100 ms with respect to the X-rays. The inset also shows a slight asymmetry towards positive delays.

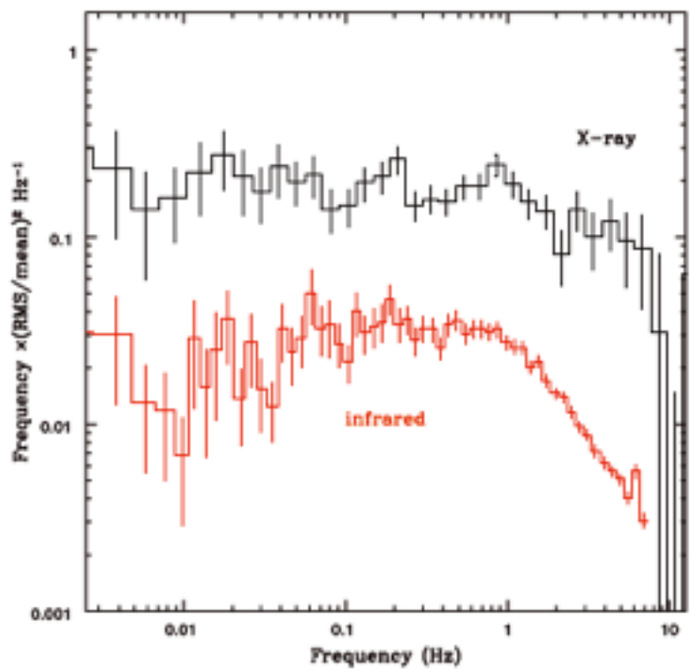

Figure 3. X-ray (2–15 keV) power spectrum of the second *RXTE* orbit (upper curve), together with the power spectrum of the simultaneous IR light curve (lower curve). The Poissonian noise has been subtracted from both the spectra. The peak at ∼6 Hz in the IR spectrum is instrumental. The high-frequency portion of the IR spectrum has yet unmodelled systematics, which however do not affect the results presented here.

Variable IR emission coming from jet near the BH, 100 ms delay wrt X-ray emission